Morphology and structure of *Homo erectus* humeri from Zhoukoudian, Locality 1 (#20899)

First revision

Editor guidance

Please submit by **20 Dec 2017** for the benefit of the authors (and your $200 publishing discount).

Structure and Criteria
Please read the 'Structure and Criteria' page for general guidance.

Raw data check
Review the raw data. Download from the materials page.

Image check
Check that figures and images have not been inappropriately manipulated.

Privacy reminder: If uploading an annotated PDF, remove identifiable information to remain anonymous.

Files

Download and review all files from the materials page.

1 Tracked changes manuscript(s)
1 Rebuttal letter(s)
4 Figure file(s)
4 Table file(s)
1 Other file(s)

For assistance email peer.review@peerj.com

Structure and Criteria

Structure your review

The review form is divided into 5 sections.
Please consider these when composing your review:

1. **BASIC REPORTING**
2. **EXPERIMENTAL DESIGN**
3. **VALIDITY OF THE FINDINGS**
4. General comments
5. Confidential notes to the editor

 You can also annotate this PDF and upload it as part of your review

When ready [submit online](#).

Editorial Criteria

Use these criteria points to structure your review. The full detailed editorial criteria is on your [guidance page](#).

BASIC REPORTING

- Clear, unambiguous, professional English language used throughout.
- Intro & background to show context. Literature well referenced & relevant.
- Structure conforms to [PeerJ standards](#), discipline norm, or improved for clarity.
- Figures are relevant, high quality, well labelled & described.
- Raw data supplied (see [PeerJ policy](#)).

EXPERIMENTAL DESIGN

- Original primary research within [Scope of the journal](#).
- Research question well defined, relevant & meaningful. It is stated how the research fills an identified knowledge gap.
- Rigorous investigation performed to a high technical & ethical standard.
- Methods described with sufficient detail & information to replicate.

VALIDITY OF THE FINDINGS

- Impact and novelty not assessed. Negative/inconclusive results accepted. *Meaningful* replication encouraged where rationale & benefit to literature is clearly stated.
- Data is robust, statistically sound, & controlled.
- Conclusions are well stated, linked to original research question & limited to supporting results.
- Speculation is welcome, but should be identified as such.

Standout reviewing tips

The best reviewers use these techniques

Tip	Example
Support criticisms with evidence from the text or from other sources	*Smith et al (J of Methodology, 2005, V3, pp 123) have shown that the analysis you use in Lines 241-250 is not the most appropriate for this situation. Please explain why you used this method.*
Give specific suggestions on how to improve the manuscript	*Your introduction needs more detail. I suggest that you improve the description at lines 57- 86 to provide more justification for your study (specifically, you should expand upon the knowledge gap being filled).*
Comment on language and grammar issues	*The English language should be improved to ensure that an international audience can clearly understand your text. Some examples where the language could be improved include lines 23, 77, 121, 128 – the current phrasing makes comprehension difficult.*
Organize by importance of the issues, and number your points	*1. Your most important issue* *2. The next most important item* *3. ...* *4. The least important points*
Please provide constructive criticism, and avoid personal opinions	*I thank you for providing the raw data, however your supplemental files need more descriptive metadata identifiers to be useful to future readers. Although your results are compelling, the data analysis should be improved in the following ways: AA, BB, CC*
Comment on strengths (as well as weaknesses) of the manuscript	*I commend the authors for their extensive data set, compiled over many years of detailed fieldwork. In addition, the manuscript is clearly written in professional, unambiguous language. If there is a weakness, it is in the statistical analysis (as I have noted above) which should be improved upon before Acceptance.*

Morphology and structure of *Homo erectus* humeri from Zhoukoudian, Locality 1

Song Xing [Corresp., 1] , Kristian J Carlson [2, 3] , Pianpian Wei [4] , Jianing He [5] , Wu Liu [1]

[1] Key Laboratory of Vertebrate Evolution and Human Origins of Chinese Academy of Sciences, Institute of Vertebrate Paleontology and Paleoanthropology, Chinese Academy of Sciences, Beijing, China

[2] Department of Integrative Anatomical Sciences, Keck School of Medicine, University of Southern California, Los Angeles, CA, USA

[3] Evolutionary Studies Institute, University of the Witwatersrand, Johannesburg, South Africa

[4] MOE Key Laboratory of Contemporary Anthropology, Collaborative Innovation Center for Genetics and Development, School of Life Sciences, Fudan University, Shanghai, China

[5] School of Archaeology and Museology, Peking University, Beijing, China

Corresponding Author: Song Xing
Email address: xingsong@ivpp.ac.cn

Background: Regional diversity in the morphology of the *H. erectus* postcranium is not broadly documented, in part, because of the paucity of Asian sites preserving postcranial fossils. Yet, such an understanding of the initial hominin taxon to spread throughout multiple regions of the world is fundamental to documenting the adaptive responses to selective forces operating during this period of human evolution.

Methods: The current study reports the first humeral rigidity and strength properties of East Asian *H. erectus* and places its diaphyseal robusticity into broader regional and temporal contexts. We estimate true cross-sectional properties of Zhoukoudian Humerus II and quantify new diaphyseal properties of Humerus III using high resolution computed tomography. Comparative data for African *H. erectus* and Eurasian Late Pleistocene *H. sapiens* were assembled, and new data were generated from two modern Chinese populations.

Results: Differences between East Asian and African *H. erectus* were inconsistently expressed in humeral cortical thickness. In contrast, East Asian *H. erectus* appears to exhibit greater humeral robusticity compared to African *H. erectus* when standardizing diaphyseal properties by the product of estimated body mass and humeral length. East Asian *H. erectus* humeri typically differed less in standardized properties from those of side-matched Late Pleistocene hominins (e.g., Neanderthals and more recent Upper Paleolithic modern humans) than did African *H. erectus*, but still often fell in the lower range of Late Pleistocene humeral rigidity or strength properties.

Discussion: Quantitative comparisons indicate that regional variability in humeral midshaft robusticity may characterize *H. erectus* to a greater extent than presently recognized. This may suggest a temporal difference within *H. erectus*, or possibly different ecogeographical trends and/or upper limb loading patterns across the taxon. Discovery and analysis of more adult *H. erectus* humeri is critical to further evaluating and potentially distinguishing between these possibilities.

1 **Title:** Morphology and structure of *Homo erectus* humeri from Zhoukoudian, Locality 1

2 **Author names:** Song Xing[1*], Kristian J. Carlson[2,3*], Pianpian Wei[4], Jianing He[5], Wu Liu[1]

3 **Author affiliations:** [1] Key Laboratory of Vertebrate Evolution and Human Origins of Chinese

4 Academy of Sciences, Institute of Vertebrate Paleontology and Paleoanthropology, Chinese

5 Academy of Sciences, Beijing, China; [2]Department of Integrative Anatomical Sciences, Keck

6 School of Medicine, University of Southern California, Los Angeles, CA, USA; [3]Evolutionary

7 Studies Institute, University of the Witwatersrand, Johannesburg, South Africa; [4] MOE Key

8 Laboratory of Contemporary Anthropology, Collaborative Innovation Center for Genetics and

9 Development, School of Life Sciences, Fudan University, Shanghai, China; [5]School of

10 Archaeology and Museology, Peking University, Beijing, China.

11 **Author email addresses:** SX (xingsong@ivpp.ac.cn), KJC (kristian.carlson@usc.edu), PW

12 (weipianpian@ivpp.ac.cn), JH (hejianing@pku.edu.cn), WL (liuwu@ivpp.ac.cn)

13 ***Corresponding Authors:** Song Xing and Kristian J. Carlson

14   **ABSTRACT**

15   **Background:** Regional diversity in the morphology of the *H. erectus* postcranium is not broadly

16   documented, in part, because of the paucity of Asian sites preserving postcranial fossils. Yet, such

17   an understanding of the initial hominin taxon to spread throughout multiple regions of the world

18   is fundamental to documenting the adaptive responses to selective forces operating during this

19   period of human evolution.

20   **Methods:** The current study reports the first humeral rigidity and strength properties of East

21   Asian *H. erectus* and places its diaphyseal robusticity into broader regional and temporal

22   contexts. We estimate true cross-sectional properties of Zhoukoudian Humerus II and quantify

23   new diaphyseal properties of Humerus III using high resolution computed tomography.

24   Comparative data for African *H. erectus* and Eurasian Late Pleistocene *H. sapiens* were

25   assembled, and new data were generated from two modern Chinese populations.

26   **Results:** Differences between East Asian and African *H. erectus* were inconsistently expressed in

27   humeral cortical thickness. In contrast, East Asian *H. erectus* appears to exhibit greater humeral

28   robusticity compared to African *H. erectus* when standardizing diaphyseal properties by the

29   product of estimated body mass and humeral length. East Asian *H. erectus* humeri typically

30   differed less in standardized properties from those of side-matched Late Pleistocene hominins

31   (e.g., Neanderthals and more recent Upper Paleolithic modern humans) than did African *H.*

32   *erectus*, but still often fell in the lower range of Late Pleistocene humeral rigidity or strength

33   properties.

34   **Discussion:** Quantitative comparisons indicate that regional variability in humeral midshaft

35   robusticity may characterize *H. erectus* to a greater extent than presently recognized. This may

36   suggest a temporal difference within *H. erectus*, or possibly different ecogeographical trends

37   and/or upper limb loading patterns across the taxon. Discovery and analysis of more adult *H.*

38   *erectus* humeri is critical to further evaluating and potentially distinguishing between these

39   possibilities.

40   **INTRODUCTION**

41   *Homo erectus* has been portrayed as a geochronologically persistent taxon encompassing

42   a great deal of regional diversity over its evolutionary history (*Antón, 2003*). The initial

43   appearance of *H. erectus* in the hominin fossil record is approximately 1.9 Ma from Koobi Fora,

44   Kenya, while the late persistence documented in Southeast Asia (i.e., Ngandong at 80 Ka) is

45   unmatched elsewhere (*Dubois, 1894, 1936; Black, 1930, 1933; von Koenigswald, 1936, 1940,*

46   *1951; Weidenreich, 1938, 1941, 1943; Woo, 1964, 1966; Chiu et al., 1973; Hu, 1973; Jacob,*

47   *1973; Santa Luca, 1980; Wu & Dong, 1982; Wu & Poirier, 1995; Swisher et al., 1996; Antón,*

48   *2003; Kaifu et al., 2005a, b; Liu et al., 2005; Zhu et al., 2008; Zaim et al., 2011*).

49   Characterization of the taxon as regionally diverse emphasizes craniodental features (*Rightmire,*

50   *1998; Antón, 2003; Kaifu et al., 2005a, b; Baab, 2008; Lordkipanidze et al. 2013; Antón et al.,*

51   *2016*) in focusing on hominin systematics (*Howells, 1980; Stringer, 1984; Rightmire, 1993;*

52   *Wood, 1994; Antón, 2002, 2003*) and feeding behaviour (*Ungar et al., 2006*). By comparison,

53   emphasis on *H. erectus* postcrania is less frequent when framing *H. erectus* diversity (*Ruff, 2008;*

54   *Pontzer et al. 2010; Puymerail et al., 2012; Ruff et al., 2015*).

55   Relative scant attention given to regional diversity in *H. erectus* postcranial fossils, in

56   part, is a function of the paucity of Asian sites preserving postcranial fossils (*Antón, 2003*); upper

57   limb elements of East Asian hominins, such as humeri, have been recovered only from

58   Zhoukoudian (see *Weidenreich, 1941*). As a result, current depictions of *H. erectus* postcranial

59   morphology draw heavily from the more abundant African, Georgian, and to a lesser extent

60   Southeast Asian, *H. erectus* fossils (e.g., *Ruff, 2008; Pontzer et al., 2010; Puymerail et al., 2012,*

61   *Ruff et al. 2015*). This work traditionally emphasizes the relatively complete immature skeleton,

62   KNM-WT 15000 (*Walker &Leakey, 1993*), a partial adult skeleton from Kenya, KNM-ER 1808

63   (*Walker et al., 1982; Leakey & Walker, 1985*), and sets of postcranial fossils from multiple

64   individuals represented at Dmanisi (*Lordkipanidze et al., 2007; Pontzer et al., 2010*).

65   Characterization of postcranial regional diversity in *H. erectus*, therefore, would benefit from

66   expanding upon these efforts to include East Asian fossils. The aim of the present study is to

67   broaden the current understanding of regional diversity in *H. erectus* by conducting the first

68   quantitative investigation of diaphyseal strength properties in East Asian *H. erectus* humeri.

69   Cross-sectional geometric properties of long bone diaphyses provide a useful means of

70   inferring activity patterns in past populations (*Ruff et al., 1993; Trinkaus et al., 1994; Trinkaus*

71   *1997; Stock, 2006; Carlson et al., 2007; Ruff, 2008; Carlson & Marchi, 2014; Ruff & Larsen,*

72   *2014, and references therein; Sládek et al., 2016*), although these inferences are not always

73   straightforward (*Pearson & Lieberman, 2004; Ruff et al., 2006; Wallace et al., 2012*). Relatively

74   recent temporal declines in humeral diaphyseal robusticity from archaic *H. sapiens* to modern *H.*

75   *sapiens* have been well-documented across Eurasia and Africa (*Ruff et al., 1993; Trinkaus et al.,*

76   *1994; Trinkaus, 1997*). Likewise, marked bilateral asymmetry in humeral strength appears to

77   have emerged in, and been more consistently expressed by, Eurasian Late Pleistocene hominins

78   compared to those of the Holocene, which is when presumed activity-related reductions have

79   been hypothesized (*Trinkaus et al., 1994; Sládek et al., 2016; Sparacello et al., 2017*).

80   Extending these humeral robusticity trends deeper into the Pleistocene hominin record

81   (e.g., *H. erectus*) has proven more challenging, among other reasons, due to the relative

82   incompleteness of the fossil record. Based on initial work, humeral strength of African *H. erectus*

83   (i.e., polar section modulus) appears to fit squarely within modern human levels of overall

84   humeral strength (*Ruff, 2008*: Fig. 2). A similar quantitative assessment of Asian *H. erectus*

85   humeral strength has not yet been performed, although levels of skeletal robusticity in more

86   recent Late Pleistocene hominins from Asia have been carefully quantified and evaluated

87   (*Shackelford, 2007; Shang & Trinkaus, 2010; Sparacello et al., 2017*). To date, evaluation of

88   humeral strength in East Asian *H. erectus* still relies largely on the original descriptions of

89   Zhoukoudian Humerus I and Humerus II published by *Weidenreich (1938, 1941)*, who remarked

90   upon the slenderness of the Humerus II shaft along with comparably more prominent muscle

91   markings on its external surface relative to modern human humeri. As with *H. erectus* femora

92   from Zhoukoudian, *Weidenreich (1938, 1941)* noted absolutely thicker cortical bone and

93   narrower (circular) medullary canals in *H. erectus* humeri as evidence of stouter shafts compared

94   to those of modern humans. *Weidenreich (1941:57)* also portrayed differences in robusticity

95   between Zhoukoudian and modern human humeral shafts as less than differences between their

96   femoral shafts, even suggesting that Zhoukoudian *H. erectus* fell within the range of modern

97   human variability in humeral robusticity.

98   Subsequent to the initial descriptions of *Weidenreich (1941)*, a third partial hominin

99   humerus (PA64, Humerus III) was recovered from Zhoukoudian Locality 1 and attributed to *H.*

100   *erectus* (*Woo & Chia, 1954*). In assessing all three humeral fossils from Zhoukoudian, *Antón*

101   *(2003)* made broad qualitative comparisons to approximately 1 Ma older African *H. erectus*

102   humeri, namely those of KNM-ER 1808 and KNM-WT 15000. *Antón (2003: 151)* noted a

103   narrower external breadth at the midshaft in Zhoukoudian humeri, presumably based on Humerus

104   II and Humerus III, and that Humerus II was "equally long, and exhibits the typically thick

105   cortical walls and reduced medullary cavity seen in African *H. erectus* fossils." This

106   characterization echoed the determination of *Weidenreich (1941)*, in part, in suggesting that

107 humeral structure of East Asian and African *H. erectus* differed from that of modern humans in

108 similar ways (i.e., thicker cortical bone and narrower medullary cavities). What remains

109 unknown, however, is whether a quantitative evaluation of humeral rigidity and strength in East

110 Asian and African *H. erectus* can corroborate this suggested equivalence, and whether humeri

111 from Zhoukoudian *H. erectus* may be truly modern human-like in their diaphyseal robusticity

112 (i.e., relative humeral rigidity and strength).

113   The goals of the present study are threefold. First, we provide the first quantitative

114 assessment of humeral rigidity and strength in East Asian *H. erectus*. Second, these new data will

115 permit the first quantitative comparisons of humeral rigidity and strength in East Asian versus

116 African *H. erectus*, which will contribute to an improved understanding of postcranial robusticity

117 and variability within the taxon overall, much as recent investigations of *H. erectus* lower limb

118 elements have (e.g., *Puymerail et al. 2012; Ruff et al. 2015*). Specifically, we address whether

119 East Asian and African *H. erectus* humeral diaphyses are similar in cortical thickness and

120 medullary cavity dimensions by quantifying their cross-sectional geometry and strength

121 properties. Comparisons between humeri of Zhoukoudian *H. erectus*, more recent Late

122 Pleistocene Eurasian hominins, and two modern Chinese populations are also undertaken in order

123 to better contextualize any potential uniqueness of Zhoukoudian humeral robusticity. Third, by

124 including two modern Chinese populations that would be expected to exhibit similar latitudinal

125 trends in ecomorphological body and limb proportions as earlier hominins from East Asia, we

126 address whether East Asian *H. erectus* may exhibit the suggested modern human-like levels of

127 humeral robusticity. In addition to providing new internal structural data for Zhoukoudian

128 Humerus II and Humerus III, we provide a new detailed description of Humerus III surface

129 morphology. This is intended to complement earlier descriptions of Humerus I and II by

130 *Weidenreich (1941)*, and to supplement an initial description of Humerus III by *Woo & Chia*

131 *(1954)*. Ultimately, the current study provides an opportunity to begin to place East Asian *H.*

132 *erectus* humeral robusticity into broader temporal and regional hominin contexts.

MATERIAL AND METHODS

134 The site of Zhoukoudian consists of a series of limestone caves approximately 50km

135 southwest of Beijing. It is situated in a transitional region between mountains and plains (*Xie et*

136 *al., 1985; Zhang, 2004*). Excavations at Zhoukoudian Cave, Locality 1 were performed between

137 1921 and 1973. Dating Locality 1 has been attempted on several occasions using a variety of

138 methods; adding the most recent cosmogenic efforts generates a potential estimated range of 0.68

139 Ma to 0.78 Ma (*Shen et al., 2009*). The Middle Pleistocene landscape of the immediate area was

140 generally similar to the present landscape. Sporopollen and sediment analyses, as well as faunal

141 composition, suggest that the surrounding area was mainly covered by forest and steppe, with

142 each of these being alternately dominant over the course of the Zhoukoudian hominin occupation

143 (*Zhang & Tang, 2007*). Hominins are thought to have occupied the cave itself, or lived near its

144 opening in a rockshelter during the Middle Pleistocene, but the overall range of cave use is

145 uncertain (*Binford et al., 1985; Weiner et al., 1998; Wu, 1999*).

146 A majority of original Zhoukoudian postcranial fossils disappeared in the 1940's, and are

147 represented today either by descriptions (e.g., *Weidenreich, 1941, 1943*) or casts produced by

148 Weidenreich. *Weidenreich (1941)* described two humeral specimens from Zhoukoudian Locality

149 1 (Humerus I and II), noting their general external rugosity compared to modern humans. Neither

150 partial humerus was associated with other skeletal elements, although *Weidenreich (1941: Table*

151 *1)* raised the possibility that Humerus II could have been associated with femur 330 (Femur III).

152 *Weidenreich (1941)* described Humerus I (specimen 81) as an unweathered small fragment of a

153   left humerus, preserving a sharp lateral supracondylar ridge and adjoining parts of the

154   anterolateral and posterior surfaces near the lateral margin of the olecranon fossa (see

155   *Weidenreich, 1941: Figs 27-29*). Based largely on the sharpness of its lateral supracondylar ridge,

156   *Weidenreich (1941)* attributed Humerus I to a male individual. *Weidenreich (1941)* described

157   Humerus II (specimen 319) as a substantial part of a left humeral diaphysis with irregular breaks

158   through the shaft approximately 20 – 30 mm distal to its surgical neck and 55 mm proximal to its

159   epicondyles (*Weidenreich, 1941*: *Figs 30-32). Weidenreich (1941)* noted its robusticity and sharp

160   surface contours, attributing it also to a male individual. *Weidenreich (1941: Fig. 31)*

161   incorporated the more fragmentary Humerus I in his reconstruction of Humerus II, which he

162   justified by pointing towards their similar external appearance and preserved proportions,

163   arriving at a reconstructed maximum length of 324 mm for the composite left humerus. In 1951,

164   a third partial hominin humerus (PA64, Humerus III) was discovered at Zhoukoudian Locality 1

165   and attributed to *H. erectus* (*Woo & Chia, 1954*). Humerus III is a right humeral fragment,

166   preserving 108.2 mm (maximum dimension) of the middle region of the shaft (Fig. 1; see Text S1

167   in Supplementary Information).

168   Insert Figure 1 here

169   *Comparative samples*

170   Zhoukoudian Humerus II and III were compared with African *H. erectus* (KNM-ER

171   1808), East Asian Late Pleistocene hominins, Middle Paleolithic modern humans, Neanderthals,

172   European early Upper Paleolithic modern humans, and East Asian Holocene modern humans.

173   Refer to Table S1 of the Supplementary Information (SI) for individual specimens included in the

174 comparative sample. Background information, such as associated dates and presumed general

175 activity patterns of groups, are briefly summarized in Text S2 of the SI when available.

176 *Acquisition of cross-sectional properties*

177   Humeri from Zhoukoudian *H. erectus*, the Late Pleistocene early modern human from

178 Tianyuan Cave, and recent modern Chinese were scanned using the 450kV high resolution

179 computed tomography facilities (designed by the Institute of High Energy Physics, Chinese

180 Academy of Sciences) housed in the Institute of Vertebrate Paleontology and Paleoanthropology

181 (IVPP). Scan parameters for the sample included: 380 kV, 1.5 mA, 4 frame averaging, 0.5

182 angular increment, and 360 degrees of rotation. Final isometric voxel size obtained for the sample

183 was 160 µm. For each scan, there were 720 projections converted into image stacks of .RAW

184 files using the IVPP225kVCT_Recon algorithm.

185   In order to quantify and compare internal structure, serial image data stacks obtained from

186 high resolution scanning were imported into VGStudio Max 2.1 (Volume Graphics GmbH,

187 Heidelberg, Germany). Using the region of interest tool, with a tolerance setting of 3000, we

188 selected all voxels representing the material of interest (i.e., a fossil or modern comparative

189 humerus). From the selected voxels, a 3D volume or region was created, and from each of these a

190 volume rendering of an entire bone was extracted. Each volume rendering of a comparative

191 specimen was aligned to the same vertical and horizontal axes *in silico* as have been used for

192 physical specimens. In other words, criteria for aligning humeral volume renderings followed

193 standard procedures used with dry bones (*Ruff, 2002a; Carlson, 2005*), and that have been

194 adapted for use in *in silico* environments (*Carlson et al., 2008*). Briefly, the longitudinal axis of a

195 rendered diaphysis was aligned to a vertical axis in morphospace. Next, each rendered volume

196   was aligned to a vertical plane passing through this vertical axis by rotating the 3D rendering

197   about its longitudinal (now also vertical) axis, or about its midpoint (i.e., rotating end over end),

198   until the two most anterior points of the distal epiphysis (i.e., usually on the capitulum and

199   trochlea of the rendering, or on both rims of the trochlea of the rendering) and the most anterior

200   projecting point on the proximal end (e.g., usually the lesser tubercle) were positioned in the

201   same vertical plane. Once specimens were aligned, intact diaphyseal cross sections were obtained

202   from the midshaft of the rendering and saved as 16-bit TIF images (Figs 2 and S1). Additional

203   details on the alignment of diaphyses and derivation of cross sections from Humerus II and

204   Humerus III are reported in the Supplementary Information (see Text S3 of the SI).

205   Insert Figure 2 here

206   Once cross sections were acquired (Fig. 2; Fig. S1), they were imported into ImageJ 1.50e

207   (*Rasband, 2015*) where they were converted to 8-bit TIFF images and standard cross-sectional

208   properties were calculated using the BoneJ 1.4.1 plugin (*Doube et al., 2010*). The only property

209   not measured using the BoneJ 1.4.1 plugin (*Doube et al., 2010*) was total subperiosteal area (TA),

210   which we measured using the magic wand tool in ImageJ 1.50e (*Rasband, 2015*). In order to pre-

211   process the 8-bit TIFFs for use in BoneJ, a three-step process was followed. First, each image

212   was binarized using a threshold for inclusion equal to the half-maximum gray value amongst

213   bone pixels. Second, the endosteal border of each cross section was cleaned (e.g., trabecular

214   struts digitally removed) following criteria outlined elsewhere (*Carlson, 2005*). Third, internal

215   spaces between endosteal and periosteal envelopes were filled, thus creating a cross section

216   without intracortical porosity.

217   For descriptive and comparative purposes, we report TA, cortical area (CA), percentage

218   cortical area (%CA), and principal moments of area (I_{max} and I_{min}). We calculate polar moment of

219   area (J) as the sum of I_{max} and I_{min}. We also report section moduli (Z_{max} and Z_{min}) and the polar

220   section modulus (Z_p). We select these properties, which are calculated independent of anatomical

221   axes, in recognition of the possibility that the fully reconstructed articular ends of the composite

222   cast of Humerus II may introduce an unknown amount of error when trying to precisely identify

223   anteroposterior (AP) and mediolateral (ML) anatomical planes during the alignment procedure

224   described above. Thus, we did not calculate any structural properties with respect to AP or ML

225   anatomical planes (i.e., I_x, I_y, Z_x, and Z_y) for either Humerus II or Humerus III.

226   *Standardization and analysis of structural properties*

227   When comparing diaphyseal cross-sectional properties of long bones across disparate

228   groups sampling different latitudes, particularly within the lower limb, it is important to

229   standardize properties by measures of body size or shape because the former may exhibit

230   allometric relationships with the latter (*Ruff et al., 1993; Ruff & Larsen, 2014*). Such standardized

231   properties are reliable and accurate measures of skeletal robusticity (see *Pearson, 2000*).

232   Typically, body mass is the most frequently used proxy for body size (or force applied when

233   modelling beam bending), while bone length is the most frequently used proxy for beam length.

234   Thus, a measure such as the product of body mass and bone length is appropriate for scaling

235   second moments of area or the polar moment of area (*Polk et al., 2000*) and section moduli (*Ruff,*

236   *2003a*) by approximating bending moments of long bones.

237   For specific interregional comparisons, such as those of East Asian and African *H. erectus*

238   properties, we followed the aforementioned rationale and standardized second moments of area,

239   polar moments of area, and section moduli using the product of estimated body mass and bone

240   length to account for any potential ecomorphological trends in body proportions. For Humerus II

241   and Humerus III, we derived body mass estimates emphasizing the average (53.6 kg) within a

242 range of ± one standard deviation (1.7 kg) calculated from multivariate body mass estimates for

243 Femur I (54.8 kg), Femur IV (54.3 kg), and Femur VI (51.6 kg) (*Grabowski et al., 2015*).

244 *Weidenreich (1941)* attributed Femur I, Femur IV, and Femur VI to male individuals, as he

245 attributed the reconstructed composite cast of Humerus II. For KNM-ER 1808, we derived an

246 estimated body mass emphasizing the average (60.2 kg) within a range of ± one standard

247 deviation (20.4 kg) calculated from three recently published estimates: 79 kg (*Will & Stock,*

248 *2014*), 63 kg (*Antón et al., 2014*: Table S2), and 38.5 kg (*Grabowski et al., 2015*). The

249 comparatively lower estimate reported by *Grabowski et al.* (2015) may be a result of their use of

250 cadaveric specimens, which have been shown to lead to equations that underestimate body mass

251 (*Ruff et al.*, in press). *Shang & Trinkaus (2010)* used vertical femoral head diameter and several

252 regression formulae to calculate a range of body mass estimates for Tianyuan 1. Ultimately, they

253 endorsed a body mass estimate of 85.1 kg for scaling limb bone structural properties of Tianyuan

254 1, which is the value we adopted in the present study. For Middle Paleolithic, Neanderthal, Early

255 Upper Paleolithic, and Late Upper Paleolithic hominins, we used body mass estimates reported

256 by *Sparacello et al. (2017)*.

257   Based on reasonably similar external dimensions and contours in their overlapping

258 regions (see Figs 1 and 2), we used estimated length of the composite Humerus II reconstruction

259 as a suitable proxy for estimated length of Humerus III. However, in acknowledgement of the

260 uncertainty that exists in estimating the length of Humerus II, and by default Humerus III, we

261 generated three different length estimates for standardizing both sets of cross-sectional properties.

262 For the first estimate, we used maximum length (324.0 mm) of the composite Humerus II

263 reconstruction published by *Weidenreich (1941)* (Figs S2 and S3). *Weidenreich (1941: 55)*

264 remarked that the proximal end of the reconstruction "may possibly have been shorter than

265 appears in the restoration." For this reason, the estimate of Weidenreich serves as a reasonable

266   upper boundary for our range of length estimates. For the second estimate, since the composite

267   Humerus II reconstruction retained the deltoid tuberosity and the proximal border of the

268   olecranon fossa, we regressed distance between the distal-most extent of the deltoid tuberosity

269   and the proximal-most extent of the olecranon fossa against maximum length in the modern

270   Chinese sample [n = 33; Maximum length = (distance between distal margin of deltoid tuberosity

271   and proximal margin of olecranon fossa)(1.544) + (133.172); p < 0.001; R-squared = 0.551; see

272   Text S4 of the SI for more details; Table S2, and Figs S2 and S4). The regression-derived

273   estimate of Humerus II maximum length is 307.4 mm. Since both modern Chinese groups,

274   particularly the Junziqing, tended to have shorter humeri than other groups in the sample, and

275   notably overlapped with the upper half of the published range for the East Eurasian Late Upper

276   Paleolithic sample (Table 1), this estimate serves as a reasonable lower boundary for our range of

277   length estimates. Finally, we averaged both of these estimates to derive a third maximum length

278   (315.7 mm). All three estimates were utilized separately when standardizing cross-sectional

279   properties, creating a range of length values (16.6 mm) equal to approximately 5.3% of the

280   average length estimate (315.7 mm). For KNM-ER 1808, we used a rough approximation of 350

281   mm for its estimated length (Ruff, 2008; pers. comm). For Tianyuan 1, we used a biomechanical

282   length of the left humerus (327.4 mm), as reported by *Shang & Trinkaus (2010)*. We used the

283   same value (327.4 mm) as a proxy for length of the right humerus of Tianyuan 1, which has not

284   yet been estimated. For Middle Paleolithic, Neanderthal, Early Upper Paleolithic, and Late Upper

285   Paleolithic hominins, we used humeral lengths reported by *Sparacello et al. (2017)*. For Datong

286   and Junziqing recent modern human samples, we measured and reported humeral maximum

287   length.

288   While some have argued that similar scaling factors should apply to the upper limb as

289   well as the lower limb, as correlations between humeral properties and body mass have been

290   demonstrated (*Ruff, 2000, 2003a*), others have argued on theoretical grounds that in humans

291   upper limb loading should be less influenced by body mass than lower limb loading since the

292   upper limbs are not habitually weight-bearing (*Pearson, 2000; Carlson et al., 2007*). In the

293   present study, since the humeral diaphysis is less likely affected by potential body breadth

294   differences compared to the proximal femur, and since many individuals within our region-

295   specific East Asian sample were without reliable body mass estimates (e.g., no associated femoral

296   head measurements), we follow others who used only bone length to standardize diaphyseal

297   properties (*Trinkaus et al., 1999*), particularly for the humerus (*Trinkaus and Churchill, 1999;*

298   *Pearson, 2000; Carlson et al., 2007*). We emphasize this additional standardization protocol

299   when conducting intraregional comparisons between Zhoukoudian *H. erectus*, Tianyuan 1, and

300   the modern Chinese samples, for whom ecomorphological trends in body or limb proportions are

301   expected to be relatively consistent. For such comparisons, we standardize cross-sectional

302   properties to create dimensionless values as follows: total area and cortical area were divided by

303   the square of maximum length, section moduli were divided by the third power of maximum

304   length, and humeral principal/polar moments of area were divided by the fourth power of

305   maximum length.

306   **RESULTS**

307   *Are East Asian and African H. erectus humeral diaphyses similar in cortical thickness and*

308   *medullary cavity dimensions?*

309   The midshaft of Humerus II exhibits a relatively high estimate of %CA similar to the

310   %CA of the KNM-ER 1808 cross section, both being near the upper end of the observed hominin

311   ranges (Tables 1 and 2). The more distal cross section of Humerus II exhibits a similar trend (i.e.,

312   2.8% lower %CA than its midshaft), still exceeding the %CA of the KNM-ER 1808 cross section

313   (Tables 2 and S3). The midshaft of Humerus III, on the other hand, is comparatively lower in

314   %CA, falling usually in the lower half of the observed hominin group ranges (i.e., between

315   observed group means and minimum values) (Table 1). While the more distal cross section of

316   Humerus III, like Humerus II, also exhibits an incremental difference in %CA compared to its

317   midshaft (0.4% lower: Tables 1 and S3), it still usually falls in the lower half of the observed

318   hominin group ranges. Due to the similarity in %CA between the two locations, only the midshaft

319   of Humerus II and Humerus III is considered further.

320   Insert Table 1 here

321   Insert Table 2 here

322   Midshaft %CAs of both Tianyuan 1 humeri fall approximately midway between the

323   observed lower Humerus III midshaft %CA and the estimated higher Humerus II midshaft %CA,

324   as do average %CAs for the Middle Paleolithic, Neanderthal, and East Eurasian Late Upper

325   Paleolithic groups (Tables 1 and 2, Fig. 3). Average %CA of the Early Upper Paleolithic group

326   also exceeds the observed %CA of the Humerus III midshaft, although by only roughly half the

327   amount of the other Late Pleistocene hominin groups. Cognizant of the generally equivalent

328   subperiosteal areas in midshaft cross sections of Humerus II and Humerus III versus the cross

329   section of the KNM-ER 1808 humerus (i.e., differences less than 5%), thicker cortical bone and a

330   relatively reduced medullary cavity best characterize Humerus II and the KNM-ER 1808

331   humerus rather than Humerus III.

332   Insert Figure 3 here

333   When standardizing the amount of bone in midshaft cross sections by squared humeral

334   length (sCA: Table S4), the range of observed Humerus III values tends to fall above sCA of

335   KNM-ER 1808. The same trend is evident when substituting the slightly greater sCA of the more

336   distal cross section of Humerus III (Tables S3 and S4). By comparison, ranges of estimated

337   Humerus II sCAs from the midshaft (Tables S5) and more distal cross section (Tables S3) fall

338   well above those of either of the other *H. erectus* humeri (Tables S3 – S5). A comparison of CAs

339   standardized to average body mass estimates largely supports the same trend where Humerus II

340   (4.25) exceeds the values exhibited by other *H. erectus* humeri: Humerus III (3.12) and KNM-ER

341   1808 (3.27) (Tables 1 and 2). With few exceptions, and irrespective of the estimated lengths used

342   as scaling factors in the present study, estimated sCAs of the Humerus II midshaft fit comfortably

343   within the upper half of observed sCA ranges for left humeri of Late Pleistocene hominins (i.e.,

344   between observed group means and maximum values) (Table S5), while observed sCAs of the

345   Humerus III midshaft tend to fall within the lower half of the observed sCA ranges for right

346   humeri of Late Pleistocene hominins (i.e., between observed group means and minimum values)

347   (Table S4). The observed sCA for the KNM-ER 1808 cross section, on the other hand, falls below

348   the observed midshaft values of both right and left Tianyuan I humeri as well as in the lower half

349   of the observed sCA ranges for right humeral midshafts of all other hominin groups in the study.

350   In other words, despite the comparatively high %CA demonstrated by KNM-ER 1808 (i.e., its

351   relatively high cortical thickness), its rather long estimated length (*Ruff, 2008*), which falls in the

352   upper end of the range of humeral lengths for the entire comparative sample analyzed in the

353   present study, results in relatively lower amounts of length-standardized compressive rigidity

354   compared to Zhoukoudian humeri.

355   *Are East Asian and African H. erectus humeral diaphyses similar in relative rigidity and*

356   *strength?*

357   Despite relatively small differences between subperiosteal areas (TA) of Zhoukoudian

358   Humerus II and Humerus III midshafts (< 3%: Tables 1 and 2), the observed differences in

359   cortical thickness create about 15% greater unstandardized principal moments of area (I_{max} and

360   I_{min}) and polar moments of area (J) in Humerus II (Tables 1 and 2). The latter structural

361   differences dissipate in the more distal cross section (< 3%), being offset by a relative increase in

362   subperiosteal area of Humerus III (Fig. 2; Table S3). This variability is noteworthy when

363   comparing all *H. erectus* humeri. Humerus III, despite exhibiting markedly less cortical thickness

364   than the humerus of KNM-ER 1808, still exhibits higher absolute I_{max}, J, and Z_{max} than KNM-ER

365   1808 (Tables 1 and S3). This indicates that Humerus III, despite its lower cortical thickness,

366   retains comparatively more absolute rigidity or strength than the humerus of KNM-ER 1808

367   largely because of its relatively minor expansion in external (subperiosteal) contour. Humerus II,

368   by comparison, exhibits comparatively greater absolute rigidity or strength both because of its

369   cortical thickness and its slightly expanded external (subperiosteal) contour.

370   Standardizing structural properties results in different trends. When standardizing humeral

371   rigidity or strength to the product of body mass and bone length, relative robusticity of

372   Zhoukoudian humeri becomes even more apparent (Tables 3 and 4). Even the less thick of the

373   two Zhoukoudian humeri (Humerus III), whether for the midshaft or the more distal cross

374   section, consistently exceeds KNM-ER 1808 in each quantitative measure irrespective of the

375   estimated length that is combined with the average estimate of body mass (Tables 3 and S4). If

376   the minimum estimate of body mass is used for standardizing properties of KNM-ER 1808,

377   Humerus III consistently falls below it, while Humerus II still slightly exceeds KNM-ER 1808 in

378   some properties (e.g., sI_{max} and sZ_{max}) and falls slightly below it in others (e.g., sI_{min}, sZ_{min}, and

379   sZ_p). Notably, KNM-ER 1808 falls near or below the lower end of comparably standardized

380   structural properties of Late Pleistocene right humeri included in the study, even when using the

381   minimum estimate of body mass (Table 3).

382   Insert Table 3 here

383   Insert Table 4 here

384   The upper end of the range of Humerus III midshaft values consistently falls at or just

385   below the sI_{max}, sZ_{max}, sJ, or sZ_p of the right Tianyuan 1 humerus (Table 3, Fig. 4, and Fig. S5),

386   while the same Humerus III ranges consistently exceed those of the less strong left Tianyuan I

387   humerus (Table 4, Fig. 4, and Fig. S5). By comparison, ranges of sI_{max}, sZ_{max}, sJ, and sZ_p

388   estimated from the Humerus II midshaft consistently exceed those observed in either Tianyuan 1

389   humerus (Tables 3 and 4, Fig. 4, and Fig. S5). Compared to right humeri from other Late

390   Pleistocene hominins (Table 3 and Fig. S5), the midshaft of Humerus III exhibits ranges of sI_{max},

391   sI_{min}, and sJ that usually overlap with the lower half of observed ranges (Neanderthals, Early

392   Upper Paleolithic modern humans, East Eurasian Late Upper Paleolithic), or falls below them

393   (Middle Paleolithic; except for sI_{max}). Compared to left humeri from other Late Pleistocene

394   hominins (Table 4 and Fig. S5), the midshaft of Humerus II exhibits ranges of sI_{max}, sI_{min}, and sJ

395   that overlap with the upper half of observed ranges (Neanderthals and Early Upper Paleolithic

396   modern humans), or usually falls above them (Middle Paleolithic and East Eurasian Late Upper

397   Paleolithic).

398   Insert Figure 4 here

399   *Does East Asian H. erectus exhibit modern human-like humeral robusticity compared to two*

400   *modern Chinese populations?*

401   *Weidenreich (1941)* described Zhoukoudian humeri as modern-like in their robusticity.

402   When comparing sCA of modern Chinese right humeri and Zhoukoudian humeri, the less robust

403   right Humerus III overlaps within the bottom half of sCA ranges of both groups (Table S4), while

404   the more robust left Humerus II overlaps with the upper half of sCA ranges of both groups

405   (Tables S4 and S5). This overlap appears to be more attributable to the comparatively thick

406   cortical shafts of both Zhoukoudian humeri rather than any sort of subperiosteal expansion since

407   even the less robust Humerus III has a %CA that falls in the upper end of the ranges observed in

408   both modern Chinese samples (Tables 1 and 2).

409   When comparing length-standardized humeral midshaft properties used to evaluate

410   rigidity or strength, Humerus II usually overlaps with the lower half of the observed Datong

411   ranges (i.e., between the observed group mean and minimum value) or falls below it, and

412   overlaps entirely with the observed lower half of the less robust Junziqing ranges (Tables S4 and

413   S5). Comparing length-standardized humeral properties of the right Humerus III to the equivalent

414   properties of the modern Chinese right humeri indicates a generally similar trend irrespective of

415   the estimated length used in scaling the former. While length-standardized properties of Humerus

416   III occasionally overlap with those in the observed Datong ranges, or more often fall below them,

417   the properties of Humerus III usually overlap entirely with the observed lower half of the less

418   robust Junziqing ranges of properties (i.e., between the observed group mean and minimum

419   value), and only occasionally extend below them (Table S4).

420   The range of humeral length estimates for Zhoukoudian Humerus II and Humerus III fall

421   in the upper half of the observed ranges for the Datong and Junziqing samples (Tables 1 and 2).

422   The Tianyuan 1 humeral length also falls in the upper half of the observed Datong and Junziqing

423   humeral length ranges (Table 1). This suggests that both modern Chinese groups may have been

424   small-bodied compared to other hominin groups in the sample, or at least appear to have had

425   comparatively short (but still strong) humeri. Regardless of which may be the case, the ranges of

426   differences exhibited by the two Zhoukoudian humeri fit within the lower half of the 2-3-fold

427   greater range of observed length-standardized properties (i.e., maximum relative to minimum

428   observed values) exhibited by these relatively numerically small groups of modern Chinese

429   (Tables S4 and S5). This underscores the amount of variability that may be exhibited by modern

430   humans, and provides quantitative support for the suggested modern-like aspects of Zhoukoudian

431   humeral robusticity (*Weidenreich, 1941*).

432   **DISCUSSION**

433   This study demonstrates that East Asian *H. erectus* humeri (Zhoukoudian Humerus II and

434   Humerus III) exhibit greater humeral rigidity and strength compared to African *H. erectus* humeri

435   (KNM-ER 1808). This difference exists whether one compares absolute values of properties, or

436   properties scaled to the product of (averages of) estimated body mass and humeral length.

437   Relative to humeri of Late Pleistocene hominins from Eurasia, the 1 Ma more recent *H. erectus*

438   humeri from Zhoukoudian, Humerus II and Humerus III, were consistently closer in robusticity

439   than the *H. erectus* humerus, KNM-ER 1808. While we could not acquire cross sections from

440   Humerus II and Humerus III in the precise diaphyseal location as acquired from KNM-ER 1808

441   (i.e., an estimated 40% length location), a second location in Zhoukoudian humeri that was distal

442   to midshaft, and also that avoided the deltoid tuberosity altogether, substantiated the midshaft

443   comparisons. Support for comparisons between the different diaphyseal locations in the present

444   study also comes from other studies (*Sládek et al., 2010; Davies & Stock, 2014; Shaw et al.,*

445   *2014; Mongle et al., 2015a, b*) that report general similarities between mid-diaphyseal cross-

446   sectional properties in human humeral or femoral cross sections sampled up to 20% length apart,

447   and that have shown mid-diaphyseal cross-sectional properties differ trivially in cross sections

448 that are approximately 5% length apart. Interestingly, the observed differences in diaphyseal

449 robusticity documented in the present study occurred despite similar cortical thicknesses in

450 KNM-ER 1808 and Humerus II and a noticeably less thick diaphysis in Humerus III. This

451 indicates that the greater subperiosteal (TA) areas of Zhoukoudian humeri (i.e., periosteal

452 expansion) were more impactful on the observed robusticity differences compared to the more

453 markedly different cortical thicknesses.

454   In considering the observed humeral robusticity differences of East Asian and African *H.*

455 *erectus*, a few factors warrant further discussion. The approximate 1 Ma difference between the

456 older African and more recent East Asian *H. erectus* humeri investigated in this study may reflect

457 temporal evolutionary trends within the taxon (apart from general body size increases) in addition

458 to any potential regional difference in body proportions or activity levels. Indeed, subsequent to

459 the discovery of KNM-ER 1808, some have proposed reassigning African *H. erectus* material to a

460 new taxon, *H. ergaster*, reflecting what is considered a different adaptive niche altogether (*Wood,*

461 *1994*). Postcranial evidence weighing in on the proposed adaptive differences between *H.*

462 *ergaster* and *H. erectus* is sparse, however, and so the current study hopes to draw deserved

463 attention to this critical issue. Discovery of contemporary *H.ergaster*/*H. erectus* humeri in Africa

464 and East Asia would shed more definitive light on the matter, as could comparisons with

465 additional *H. erectus* humeri from other geographic regions (e.g., West Asia and Southeast

466 Asia).In the interim, it is worthwhile to consider potential differences in body proportions across

467 individuals from these regions since they may introduce a potential confound in comparisons of

468 humeral robusticity. Latitudinal clines in body proportions (i.e., Allen's rule) have been well-

469 documented in extinct and extant hominins (*Allen, 1877; Ruff, 1994; Holliday, 1997; Tilkens et*

470 *al., 2007; Ruff, 2010*). Specifically, equatorial human populations, such as those from Africa, tend

471 to have more linear body shapes and longer limbs relative to body mass compared to human

472   populations from higher latitudes (e.g., the modern Chinese populations investigated in the

473   present study), although aspects of environmental quality (e.g., nutritional differences) may

474   modulate the phenotypic expression of these differences to some extent (*Katzmarzyk & Leonard,*

475   *1998; Bogin et al., 2002; Bogin & Varela-Silva, 2010*). This ecomorphological trend may

476   characterize hominin body plans at least as early as archaic *H. sapiens* from the Middle

477   Pleistocene of different regions, including East Asia (*Trinkaus et al., 1999; Ruff, 2002b;*

478   *Rosenberg et al., 2006*). While a portion of the observed differences between the size-

479   standardized properties of Humerus II and Humerus III versus KNM-ER 1808 may be

480   attributable to overall differences in *H. erectus* body size and limb proportions, such as would be

481   manifested in humeral length, we attempted to control for this possibility by also incorporating

482   estimates of body mass in these scaling factors. Thus, our estimates of comparative humeral

483   robusticity in *H. erectus* reflect rigidity or strength *after* controlling for potential differences in

484   estimated body size and limb length of individuals.

485   In addition to these observed differences in humeral diaphyseal robusticity, diaphyseal

486   shapes of Humerus II and Humerus III diverged from that of the humerus of KNM-ER 1808 (i.e.,

487   the latter exhibited comparatively more equivalent I_{max} and I_{min} values; Tables 1 and 2 and Fig. 2),

488   possibly hinting at potential differences in upper limb use. Additional suitable adult *H. erectus*

489   humeri from both regions would be needed in order to rigorously investigate this possibility

490   further. Involvement of the upper limb in activities associated with selective advantages for

491   hominins, and thus those that could be potentially worth future investigation in order to

492   contextualize the observed differences in humeral diaphyseal robusticity or shape, include

493   projectile throwing (*Roach et al., 2013; Roach and Richmond, 2015*), throwing in general (*Shaw*

494   *& Stock, 2009; Warden et al., 2009*), spear thrusting (*Schmitt et al., 2003*), stone tool

495   manufacturing (*Rolian et al., 2011; Williams et al., 2012; Key & Dunmore, 2015*), and scraping

496   (*Shaw et al., 2012*). While some (*Roach et al., 2013; Roach & Richmond, 2015*) have attributed

497   morphological evidence of projectile throwing to *H. erectus* (e.g., low humeral torsion, a human-

498   like laterally-oriented scapular glenoid, and a tall mobile waist), there is no documented evidence

499   of projectile use or throwing at Zhoukoudian, Locality 1. Unimanual scraping tasks, such as hide

500   preparation, have been argued to generate bilateral asymmetry in upper limb muscle activity

501   (*Shaw et al., 2012*), making it notable that side scrapers are the most abundant artifact in the

502   Locality 1 archaeological assemblage (*Pei & Zhang, 1985; Zhang, 2004; Li et al., 2011*). To date,

503   however, experimental assessments of loading associated with stone tool use and manufacturing

504   focus on the hand rather than the forearm or arm (*Rolian et al., 2011; Williams et al., 2012; Key*

505   *& Dunmore, 2015*). The role these activities, or others, may have in inducing the dramatic right-

506   side dominant asymmetry observed in diaphyseal strength of Late Pleistocene hominins in

507   general (*Sládek et al., 2016; Sparacello et al., 2017*), or the Late Pleistocene hominin, Tianyuan

508   I, in particular (*Shang et al., 2007; Shang & Trinkaus, 2010*), also remain unclear. Thus, caution

509   is warranted when assessing right and left humeri from Zhoukoudian for potential activity-related

510   bilateral asymmetry.

511   While *Weidenreich (1941)* may have emphasized external surface comparisons in

512   describing the 'thicker' Humerus II as modern human-like in its robusticity, quantitative

513   evaluation of internal structure supports this assessment of its humeral robusticity. Evaluation of

514   Humerus III further corroborates the suggested similarity. Despite relative cortical thicknesses of

515   Humerus II and Humerus III (%CA) exceeding those of the majority of individuals in both

516   modern Chinese samples investigated in the study, which themselves were characterized by

517   comparatively robust but short humeri, comparatively expanded subperiosteal areas of the

518   modern Chinese humeri appear to be responsible for their typically higher measures of length-

519   standardized humeral robusticity.

520   In the Late Pleistocene of Southeast Asia, comparatively smaller body sizes and statures

521   have been reported compared to contemporaneous regional populations from Africa and Europe

522   (*Shackelford, 2007*). The comparatively short humeri of both modern Chinese samples (i.e.,

523   Datong and Junziqing) suggest that these populations also may have been relatively small-bodied,

524   or at least that they were characterized by short humeri. Both modern Chinese samples exhibited

525   length-standardized humeral robusticity (e.g., sJ or sZ_p) that bracketed that of the Late

526   Pleistocene Tianyuan 1 hominin either in the upper half (Jinziqing) or lower half (Datong) of

527   their observed ranges. Body mass of Tianyuan 1 has been estimated as 85.1 kg (*Shang &*

528   *Trinkaus, 2010*). Both modern Chinese populations also exhibited observed ranges of length-

529   standardized humeral robusticity that broadly overlapped with those of individuals comprising

530   the East Eurasian Late Upper Paleolithic (i.e., Minatogawa and Tam Hang). Average body mass

531   estimates for these individuals has been estimated as 51.4 kg, with a range of 42.3 to 70.5 kg

532   (Table 1). Assuming general equivalence, or even minimal divergence in body sizes, both modern

533   Chinese populations appear to have been characterized by less dramatic declines in humeral

534   robusticity from Late Pleistocene levels compared to what is typically observed in Holocene

535   populations (*Ruff et al., 1993; Trinkaus et al., 1994; Trinkaus, 1997; Ruff et al. 2015*).

536   There are a few limitations in the current study that bear mention. We used anatomical

537   markers to identify diaphyseal locations in our East Asian sample (e.g., distal-most border of

538   deltoid insertion), as one often is resigned to relying upon when analysing fossils that do not

539   preserve entire bone lengths. This may have resulted in a small amount of imprecision when

540   comparing diaphyseal locations. We also had to estimate medullary cavity size and dimensions in

541   Humerus II. While *Weidenreich (1941: Fig. 58 D)* provided information on relative size of the

542   cavity, this was only in a single dimension so we had to assume similarity in form to Humerus III.

543   Nonetheless, the periosteal border is more impactful on cross-sectional properties than the

544   endosteal border, as the current study demonstrates. While we used a range of length estimates

545   for Humerus II to standardize properties for Humerus III, reasonably similar external contours of

546   both humeri (see Figs 1 and 2) suggest that the actual length of Humerus III probably fell within

547   or close to this range of values. We were unable to assess the degree of bilateral asymmetry

548   expressed in Zhoukoudian *H. erectus* humeri, which is noteworthy since the left Humerus II

549   consistently exceeded the right Humerus III in structural properties. This is opposite the trend

550   typically expressed in Late Pleistocene hominins preserving both humeri (e.g., consider Tianyuan

551   1), suggesting perhaps they represent two individuals.

552   Variability in published body mass estimates of KNM-ER 1808 and its purported

553   pathological condition also bear further mention in this discussion. A two-fold range of body mass

554   estimates attributed to KNM-ER 1808 have been recently published: 38.5 kg to 79 kg (*Will &*

555   *Stock, 2014*; *Antón et al., 2014*; *Grabowski et al., 2015*). The comparatively low most recent

556   estimate of body mass, 38.5 kg (*Grabowski et al.,* 2015), which we incorporated in our

557   conservative use of an average estimate, may be an underestimate due to the authors' reliance on

558   cadavers in generating the original regression estimation equation (see *Ruff et al. 2018*). If this

559   estimate were more in line with the other higher published estimates, it would only further

560   accentuate the comparatively lower robusticity of the KNM-ER 1808 humerus observed here.

561   Alternatively, even when using such a low estimate of body mass (i.e., one standard deviation

562   below our average estimate), Humerus II still slightly exceeds KNM-ER 1808 in a few aspects of

563   humeral robusticity (e.g., sI_{max}, sZ_{max}, and sJ). Ultimately, we believe the use of an average

564   estimate of body mass was the most conservative approach. *Ruff (2008)* noted that reactive bone

565   formation on diaphyseal surfaces of KNM-ER 1808 could be differentiated from the original

566   periosteal borders, lending confidence to the accuracy of calculating structural properties from

567   the humeral diaphysis. However, the extent to which the condition responsible for the reactive

568   bone formation may have altered the activity profile of the individual remains unknown, although

569   presumably upper limb activities would have been impacted less than lower limb activities due to

570   less reactive bone formation on the former.

571   Finally, the observed length-standardized robusticity displayed by modern Chinese

572   samples (Datong and Junziqing) relies on their body size estimates not dramatically exceeding

573   those of Late Pleistocene hominins in the region (e.g., individuals from Tianyuan Cave,

574   Minatogawa, and Tam Hang). Smaller body sizes of the modern Chinese samples would only

575   further enhance their robusticity. While a broader regional study of East Asian Holocene

576   populations is beyond the scope of the current study, such a study would be necessary to better

577   understand whether the Datong and Junziqing may be representative of regional trends.

578   **CONCLUSIONS**

579   Consistent differences were observed between the more robust humeri of East Asian *H.*

580   *erectus* (Zhoukoudian Humerus II and Humerus III) compared to the less robust humerus of

581   African *H. erectus* (KNM-ER 1808). Zhoukoudian Humerus II and Humerus III also resembled

582   Late Pleistocene hominins in humeral robusticity to a greater extent than the 1 Ma older KNM-

583   ER 1808 humerus. This indicates the presence of regional differences in *H. erectus* humeral

584   structure, which may reflect temporal trends (e.g., between *H. ergaster* versus *H. erectus*),

585   ecogeographic trends in body proportions, and/or potential activity-related differences.

586   Contemporaneous *H. erectus* fossils from each region could begin to help resolve these non-

587   mutually exclusive possibilities. Two modern Chinese samples also exhibited increased or

588   equivalent humeral robusticity compared to *H. erectus* (Zhoukoudian Humerus II and Humerus

589   III) and Late Pleistocene hominins from Asia (Tianyuan Cave 1, Minatogawa, and Tam Hang).

590   Thus, quantitative evaluation of internal humeral structure supports the original description by

591   *Weidenreich* (*1941*) of modern human-like robusticity of the Zhoukoudian Humerus II based on

592   its external surface. A similar investigation of Zhoukoudian Humerus III provides corroborating

593   support.

594   **ACKNOWLEDGEMENTS**

600   **Data Availability**

601   The following information was supplied regarding data availability: Part of the data has

602   been supplied as Supplementary File.

603   **REFERENCES**

604   **Allen JA. 1877.** The influence of physical conditions in the genesis of species. *Radical Review* **1**:

605   108-140.

606   **Antón SC. 2002.** Evolutionary significance of cranial variation in Asian *Homo erectus*.

607   *American Journal of Physical Anthropology* **118**:301-323. DOI: 10.1002/ajpa.10091

608   **Antón SC. 2003.** The natural history of *Homo erectus*. *Yearbook of Physical Anthropology*

609   **46**:126-170. DOI: 10.1002/ajpa.10399

610   **Antón SC, Potts R, Aiello LC. 2014.** Evolution of early *Homo*: an integrated biological

611   perspective. *Science* **345**:1236828-1 – 1236828-13. DOI: 10.1126/science.1236828

612   **Antón SC, Taboada HG, Middleton ER, Rainwater CW, Taylor AB, Turner TR, Turnquist**

613   **JE, Weinstein KJ, Williams SA. 2016.** Morphological variation in Homo erectus and the

614   origins of developmental plasticity. *Philosophical Transactions of the Royal Society of*

615   *London. Series B, Biological Science* **371**: 20150236. DOI: 10.1098/rstb.2015.0236

616   **Baab KL. 2008.** The taxonomic implications of cranial shape variation in *Homo erectus*. *Journal*

617   *of Human Evolution* **54**: 827-847. https://doi.org/10.1016/j.jhevol.2007.11.003

618   **Binford LR, Ho CK, Aigner JS, Alimen M-H, Borrero LA, Te-K'un C, Chung T, Goldberg**

619   **P, Ikawa-Smith F, Lanata JL, Zune L, Luchterhand K, Lyman RL, Goñalons GM, Pei G,**

620   **Straus LG, Yacobaccio HD, Yi S. 1985.** Taphonomy at a Distance: Zhoukoudian, "The cave

621   home of Beijing Man"? *Current Anthropology* **2**: 413-442. https://doi.org/10.1086/203303

622   **Black D. 1930.** *On an adolescent skull of* Sinanthropus pekinensis *in comparison with an adult*

623   *skull of the same species and with other hominid skulls, recent and fossil.* Palaeontogia Sinica

624   Series D **7**: 1-114.

625   **Black D. 1933.** *Sinanthropus* skeletal remains, etc. In part II of "Fossil Man in China." Geolog.

626   Memoirs, Series A No.11, pp. 63-109.

627   **Bogin B, Smith P, Orden AB, Varela Silva MI, Loucky J. 2002.** Rapid change in

628   height and body proportions of Maya American children. *American Journal of Human*

629   *Biology* **14**: 753-761.

630   **Bogin B, Varela-Silva MI. 2010.** Leg length, body proportion, and health: a review

631   with a note on beauty. *International Journal of Environmental Research & Public Health* **7**:

632   1047-1075.

633   **Carlson KJ. 2005.** Investigating the form-function interface in African apes – relationships

634   between principal moments of area and positional behaviors in femoral and humeral

635   diaphyses. *American Journal of Physical Anthropology* **127**: 312-334. DOI:

636   10.1002/ajpa.20124

637   **Carlson KJ, Grine FE, Pearson OM. 2007.** Robusticity and sexual dimorphism in the

638   postcranium of modern hunter-gatherers from Australia. *American Journal of Physical*

639   *Anthropology* **134**: 9-23. DOI: 10.1002/ajpa.20617

640   **Carlson KJ, Marchi D. (Eds). 2014.** *Reconstructing mobility – environmental, behavioral, and*

641   *morphological determinants*. Springer Press, New York.

642   **Carlson KJ, Sumner DR, Morbeck ME, Nishida T, Yamanaka A, Boesch C. 2008.** Role of

643   nonbehavioral factors in adjusting long bone diaphyseal structure in free-ranging *Pan*

644   *troglodytes*. *International Journal of Primatology* **29**: 1401-1420.

645   **Chiu CL, Gu YM, Zhang YY, Chang SS. 1973.** Newly discovered *Sinanthropus* remains and

646   stone artefacts at Choukoutien. *Vertebrata Palasiatica* **11**: 109-131.

647   **Churchill SE. 1994.** *Human upper body evolution in the Eurasian Later Pleistocene*. University

648   of New Mexico.

649 **Davies TG, Stock JT. 2014.** Human variation in the periosteal geometry of the lower limb:

650   signatures of behaviour among human Holocene populations. In: Carlson, K.J., Marchi, D.,

651   (Eds), *Reconstructing mobility – environmental, behavioral, and morphological determinants*.

652   Springer Press, New York. pp 67-90.

653 **Doube M, Klosowski MM, Arganda-Carreras I, Cordeliéres F, Dougherty RP, Jackson J,**

654   **Schmid B, Hutchinson JR, Shefelbine SJ. 2010.** BoneJ: free and extensible bone image

655   analysis in ImageJ. *Bone* **47**:1076-1079. https://doi.org/10.1016/j.bone.2010.08.023

656 **Dubois E. 1894.** Pithecanthropus erectus*: eine menschenähnliche Übergangsform aus Java.*

657   Landesdruckerei, Batavia.

658 **Dubois E. 1936.** Racial identity of *Homo soloensis* Oppenoorth (including *Homo modjokertensis*

659   von Koenigswald and *Sinanthropus pekinensis* Davidson Black). Koninklijke Akademie van

660   Wetenschappen, *Amsterdam* **34**: 1180–1185.

661 **Grabowski M, Hatala KG, Jungers WL, Richmond BG. 2015.** Body mass estimates of

662   hominin fossils and the evolution of human body size. *Journal of Human Evolution* **85**: 75-93.

663   https://doi.org/10.1016/j.jhevol.2015.05.005

664 **Howells WW. 1980.** *Homo erectus* – who, when, and where: A survey. *Yearbook of Physical*

665   *Anthropology* **23**: 1-23. DOI: 10.1002/ajpa.1330230503

666 **Holliday TW. 1997.** Body proportions in Late Pleistocene Europe and modern human origins.

667   *Journal of Human Evolution* **32**: 423-447. https://doi.org/10.1006/jhev.1996.0111

668 **Hu CZ. 1973.** Ape-man teeth from Yuanmou, Yunnan. *Acta Geological Sinica* **1**, 65-72.

669   **Jacob T. 1973.** Palaeoanthropological discoveries in Indonesia with special reference to the finds

670   of the last two decades. *Journal of Human Evolution* **2**: 473-485. https://doi.org/10.1016/0047-

671   2484(73)90125-5

672   **Kaifu Y, Aziz F, Baba H. 2005a.** Hominid mandibular remains from Sangiran: 1952-1986

673   Collection. *American Journal of Physical Anthropology* **128**: 497-519. DOI:

674   10.1002/ajpa.10427

675   **Kaifu Y, Baba H, Aziz F, Indriati E, Schrenk F, Jacob T. 2005b.** Taxonomic affinities and

676   evolutionary history of the Early Pleistocene hominids of Java: dentognathic evidence.

677   *American Journal of Physical Anthropology* **128**: 709-726. DOI: 10.1002/ajpa.10425

678   **Katzmarzyk PT, Leonard WR. 1998.** Climatic influences on human body size and

679   proportions: ecological adaptations and secular trends. *American Journal of Physical*

680   *Anthropology* **106**: 483-503. DOI: 10.1002/(SICI)1096-8644(199808)106:4<483::AID-

681   AJPA4>3.0.CO;2-K

682   **Key AJM, Dunmore CJ. 2015.** The evolution of the hominin thumb and the influence exerted

683   by the non-dominant hand during stone tool production. *Journal of Human Evolution* **78**: 60-

684   69. https://doi.org/10.1016/j.jhevol.2014.08.006

685   **Langbroek M, Roebroeks W. 2000.** Extraterrestrial evidence on the age of the hominids from

686   Java. *Journal of Human Evolution* **38**, 595-600.

687   **Leakey REF, Walker AC. 1985.** Further hominids from the Plio-Pleistocene of Koobi Fora,

688   Kenya. *American Journal of Physical Anthropology* **67**: 135-163.

689   DOI: 10.1002/ajpa.1330670209

690   **Li F, Wang CX, Liu DC, Zhang XL, Zhang SQ, Gao X. 2011.** Vein quartz procurement at

691   Layer 4~5 of the Zhoukoudian Locality 1. *Quaternary Science* **31**: 900-908.

692   **Liu W, Zhang Y, Wu X. 2005.** A middle Pleistocene human cranium from Tangshan, Nanjing of

693   southeast China: a comparison with *Homo erectus* from Eurasia and Africa based on new

694   reconstruction. *American Journal of Physical Anthropology* **25**: 253-262. DOI:

695   10.1002/ajpa.20066

696   **Lordkipanidze D, Jashashvili T, Vekua A, Ponce de León MS, Zollikofer CPE, Rightmire**

697   **GP, Pontzer H, Ferring R, Oms O, Tappen M, Bukhsianidze M, Agusti J, Kahlke R,**

698   **Kiladze G, Martinez-Navarro B, Mouskhelishvili A, Nioradze M, Rook L. 2007.**

699   Postcranial evidence from early *Homo* from Dmanisi, Georgia. *Nature* **449**: 305-310.

700   **Lordkipanidze D, de León MSP, Margvelashvili A, Rak Y, Rightmire GP, Vekua A,**

701   **Zollikofer CP. 2013.** A complete skull from Dmanisi, Georgia, and the evolutionary biology

702   of early *Homo*. *Science* **342**: 326-331. DOI: 10.1126/science.1238484

703   **Macintosh AA, Davies TG, Ryan TM, Shaw CN, Stock JT. 2013.** Periosteal versus true cross-

704   sectional geometry: a comparison along humeral, femoral, and tibial diaphyses. *American*

705   *Journal of Physical Anthropology* **150**: 442-452. DOI: 10.1002/ajpa.22218

706   **Mongle CS, Wallace IJ, Grine FE. 2015a.** Cross-sectional structural variation relative to

707   midshaft along hominin diaphyses. II. The forelimb. *American Journal of Physical*

708   *Anthropology* **158**: 386-397. DOI: 10.1002/ajpa.22802

709   **Mongle CS, Wallace IJ, Grine FE. 2015b.** Cross-sectional structural variation relative to

710   midshaft along hominin diaphyses. II. The hind limb. *American Journal of Physical*

711   *Anthropology* **158**: 398-407. DOI: 10.1002/ajpa.22802

712   **Mott RL. 1996.** Applied strength of materials. 3rd ed. Upper Saddle River, NJ: Prentice Hall, Inc.

713   **Pearson OM. 2000.** Activity, climate, and postcranial robusticity. *Current Anthropology* **41**: 569-

714   609. https://doi.org/10.1086/317382

715   **Pearson OM, Lieberman DE. 2004.** The aging of "Wolff's Law": ontogeny and responses to

716   mechanical loading in cortical bone. Yearbook of Physical Anthropology **47**, 63-99.

717   **Pei WZ, Zhang SS. 1985.** A study on the lithic artifacts of *Sinanthropus*. Palaeontogia Sinica

718   New Series D **12**:1-277.

719   **Polk JD, Demes B, Jungers WL, Biknevicius AR, Heinrich RE, Runestad JA. 2000.** A

720   comparison of primate, carnivoran and rodent limb bone cross-sectional properties: are

721   primates really unique? *Journal of Human Evolution* **29**: 297-325.

722   https://doi.org/10.1006/jhev.2000.0420

723   **Pontzer H, Rolian C, Rightmire GP, Jashashvili T, Ponce de León MS, Lordkipanidze D,**

724   **Zollikofer CPE. 2010.** Locomotor anatomy and biomechanics of the Dmanisi hominins.

725   *Journal of Human Evolution* **58**: 492-504. https://doi.org/10.1016/j.jhevol.2010.03.006

726   **Puymerail L, Ruff CB, Bondioli L, Widianto H, Trinkaus E, Macchiarelli R. 2012.**

727   Structural analysis of the Kresna 11 *Homo erectus* femoral shaft (Sangiran, Java). *Journal of*

728   *Human Evolution* **63**:741-749. https://doi.org/10.1016/j.jhevol.2012.08.003

729   **Rasband WS. 1997-2015.** ImageJ, U.S. National Institutes of Health, Bethesda, Maryland, USA,

730   http://imagej.nih.gov/ij/.

731   **Rightmire GP. 1993.** *The evolution of* Homo erectus. Cambridge University Press, New York.

732   **Rightmire GP. 1998.** Evidence from facial morphology for similarity of Asian and African

733   representatives of *Homo erectus*. *American Journal of Physical Anthropology* **106**: 61-85.

734   DOI: 10.1002/(SICI)1096-8644(199805)106:1<61::AID-AJPA5>3.0.CO;2-G

735   **Roach NT, Venkadesan M, Rainbow MJ, Lieberman DE. 2013.** Elastic energy storage in the

736   shoulder and the evolution of high-speed throwing in *Homo*. *Nature* **498**: 483-487.

737   DOI:10.1038/nature12267

738   **Roach NT, Richmond BG. 2015.** Clavicle length, throwing performance and the reconstruction

739   of the *Homo erectus* shoulder. *Journal of Human Evolution* **80**: 107-113.

740   https://doi.org/10.1016/j.jhevol.2014.09.004

741   **Rolian C, Lieberman DE, Zermeno JP. 2011.** Hand biomechanics during simulated stone tool

742   use. *Journal of Human Evolution* **61**: 26-41. https://doi.org/10.1016/j.jhevol.2011.01.008

743   **Rosenberg KR, Lü Z, Ruff CB. 2006.** Body size, body proportions and

744   encephalization in a Middle Pleistocene archaic human from northern China. DOI:

745   10.1073/pnas.0508681103*Proceedings of the National Academy of Sciences of the United*

746   *States of America* **103**: 3552-3556.

747   **Ruff CB, Burgess ML, Squyres N, Junno J-A, Trinkaus E. In press.** Lower limb articular

748   scaling and body mass estimation in Pliocene and Pleistocene hominins. *Journal of*

749   *Human Evolution.*

750   **Ruff CB. 1994.** Morphological adaptation to climate in modern and fossil hominids.

751   *Yearbook of Physical Anthropology* **37**: 65-107. DOI: 10.1002/ajpa.1330370605

752   **Ruff CB. 2000.** Body size, body shape, and long bone strength in modern humans. *Journal of*

753   *Human Evolution* **38**: 269-290. https://doi.org/10.1006/jhev.1999.0322

754   **Ruff CB. 2002a.** Long bone articular and diaphyseal structure in Old World monkeys and apes. I:

755   locomotor effects. *American Journal of Physical Anthropology* **119**: 305-342. DOI:

756   10.1002/ajpa.10117

757   **Ruff CB. 2002b.** Variation in human body size and shape. *Annual Review of*

758   *Anthropology* **31**: 211-232. https://doi.org/10.1146/annurev.anthro.31.040402.085407

759   **Ruff CB. 2003a.** Growth in bone strength, body size, and muscle size in a juvenile longitudinal

760   sample. *Bone* **33**: 317-329. https://doi.org/10.1016/S8756-3282(03)00161-3

761   **Ruff CB. 2003b.** Ontogenetic adaptation to bipedalism: age changes in femoral to humeral length

762   and strength proportions in humans, with a comparison to baboons. *Journal of Human*

763   *Evolution* **45**: 317-349. https://doi.org/10.1016/j.jhevol.2003.08.006

764   **Ruff CB. 2008.** Femoral/humeral strength in early African *Homo erectus*. *Journal of Human*

765   *Evolution* **54**:383-390. https://doi.org/10.1016/j.jhevol.2007.09.001

766   **Ruff CB. 2009.** Relative limb strength and locomotion in *Homo habilis*. *American Journal of*

767   *Physical Anthropology* **138**: 90-100. DOI: 10.1002/ajpa.20907

768   **Ruff CB. 2010.** Body size and body shape in early hominins – implications of the Gona pelvis.

769   *Journal of Human Evolution* **58**: 166-178. https://doi.org/10.1016/j.jhevol.2009.10.003

770   **Ruff CB, Puymerail L, Macchiarelli R, Sipla J, Ciochon RL. 2015.** Structure and

771   composition of the Trinil femora: functional and taxonomic implications. *Journal of Human*

772   *Evolution* **80**:147-158. https://doi.org/10.1016/j.jhevol.2014.12.004

773   **Ruff CB., Holt B, Niskanen M, Sladek V, Berner M, Garofalo E, Garvin HM, Hora M,**

774   **Junno J-A, Schuplerova E, Vilkama R, Whitney E. 2015.** Gradual decline in mobility with

775   the adoption of food production in Europe. *Proceedings of the National Academy of Sciences*

776   *of the United States of America* **112**: 7147-7152. DOI: 10.1073/pnas.1502932112

777   **Ruff CB, Holt B, Trinkaus E. 2006.** Who's afraid of the big bad Wolff?: Wolff's Law" and bone

778   functional adaptation. *American Journal of Physical Anthropology* **129**: 484-498. DOI:

779   10.1002/ajpa.20371

780   **Ruff CB, Larsen CS. 2014.** Long bone structural analyses and the reconstruction of past

781   mobility: a historical review. In: Carlson, K.J., Marchi, D., (Eds), *Reconstructing mobility –*

782   *environmental, behavioral, and morphological determinants*. Springer Press, New York. pp

783   13-30.

784   **Ruff CB, Trinkaus E, Walker A, Larsen CS. 1993.** Postcranial robusticity in *Homo*. I:

785   Temporal trends and mechanical interpretation. *American Journal of Physical Anthropology*

786   **91**: 21-53. DOI: 10.1002/ajpa.1330910103

787   **Ruff CB, Walker A. 1993.** Body size and body shape. In: Walker, A., Leakey, R. (Eds.). *The*

788   *Nariokotome Homo erectus skeleton*. Harvard University Press, Cambridge, pp. 234-265.

789   **Santa Luca AP. 1980.** *The Ngandong fossil hominids*. Department of Anthropology, Yale

790   University, New Haven.

791   **Schmitt D, Churchill SE, Hylander WL. 2003.** Experimental evidence concerning spear use in

792   Neanderthals and early modern humans. *Journal of Archaeological Science* **30**: 103-114.

793   https://doi.org/10.1006/jasc.2001.0814

794   **Shackelford LL. 2007.** Regional variation in the postcranial robusticity of Late Upper

795   Paleolithic humans. *American Journal of Physical Anthropology* **133**: 655-668. DOI:

796   10.1002/ajpa.20567

797   **Shang H, Tong H, Zhang S, Chen F, Trinkaus E. 2007.** An early modern human from Tianyuan

798   Cave, Zhoukoudian, China. *Proceedings of the National Academy of Sciences of the United*

799   *States of America* **104**: 6573-5678. DOI: 10.1073/pnas.0702169104

800   **Shang H, Trinkaus E. 2010.** *The early modern human from Tianyuan Cave, China*. Texas A&M

801   University Press, College Station, TX.

802   **Shaw CN, Hofmann CL, Petraglia MD, Stock JT, Gottschall JS. 2012.** Neanderthal humeri

803   may reflect adaptation to scraping tasks, but not spear thrusting. *PLoS One* **7**: e40349.

804   https://doi.org/10.1371/journal.pone.0040349

805   **Shaw CN, Stock JT. 2009.** Habitual throwing and swimming correspond with upper limb

806   diaphyseal strength and shape in modern human athletes. *American Journal of Physical*

807   *Anthropology* **140**: 160-172. DOI: 10.1002/ajpa.21063

808   **Shaw CN, Stock JT, Davies TG, Ryan TM. 2014.** Does the distribution and variation in cortical

809   bone along the lower limb diaphyses reflect selection for locomotor economy. In: Carlson,

810   K.J., Marchi, D., (Eds), *Reconstructing mobility – environmental, behavioral, and*

811   *morphological determinants*. Springer Press, New York. pp 49-66.

812   **Shen G, Gao X, Gao B, Granger DE. 2009.** Age of Zhoukoudian *Homo erectus* determined

813   with ^{26}Al/^{10}Be burial dating. *Nature* **458**: 198-200.

814   **Sládek V, Berner M, Galeta P, Friedl L, Kudrnová Š. 2010.** Technical note: the effect of

815   midshaft location on the error ranges of femoral and tibial cross-sectional parameters.

816   *American Journal of Physical Anthropology* **141**: 325-332. DOI: 10.1002/ajpa.21153

817   **Sládek V, Ruff CB, Berner M, Holt B, Niskanen M, Schuplerová E, Hora M. 2016.** The

818   impact of subsistence changes on humeral bilateral asymmetry in Terminal Pleistocene and

819   Holocene Europe. *Journal of Human Evolution* **92**: 37-49.

820   https://doi.org/10.1016/j.jhevol.2015.12.001

821   **Sparacello VS, Villotte S, Shackelford LL. Trinkaus E. 2016.** Patterns of humeral asymmetry

822   among Late Pleistocene humans. *Comptes Rendus Palevol* **16**: 680-689.

823   http://dx.doi.org/10.1016/j.crpv.2016.09.001.

824   **Stock JT. 2006.** Hunter-gatherer postcranial robusticity relative to patterns of mobility, climatic

825   adaptation and selection for tissue economy. *American Journal of Physical Anthropology* **131**:

826   194-204. DOI: 10.1002/ajpa.20398

827   **Stock JT, Shaw CN. 2007.** Which measures of diaphyseal robusticity are robust? A comparison

828   of external methods of quantifying the strength of long bone diaphysis to cross-sectional

829   geometric properties. *American Journal of Physical Anthropology* **134**: 412-423. DOI:

830   10.1002/ajpa.20686

831   **Stringer CB. 1984.** The definition of *Homo erectus* and the existence of the species in Africa and

832   Europe. *Courier Forschungsinstitut Senckenberg* **9**: 131-143.

833   **Swisher CC III, Rink WJ, Antón SC, Schwarcz HP, Curtis GH, Widiasmoro AS. 1996.**

834   Latest *Homo erectus*, in Java: potential contemporaneity with *Homo sapiens* in Southeast Asia.

835   *Science* **274**: 1870-1874.

836   **Tilkens MJ, Wall-Scheffler C, Weave TD, Steudel-Numbers K. 2007.** The effects of body

837   proportions on thermoregulation: an experimental assessment of Allen's rule. *Journal of*

838   *Human Evolution* **53**: 286-291. https://doi.org/10.1016/j.jhevol.2007.04.005

839   **Tong H, Shang H, Zhang S, Chen F. 2004.** A preliminary report on the newly found Tianyuan

840   Cave, a Late Pleistocene human fossil site near Zhoukoudian. *Chinese Science Bulletin* **49**:

841   853-857.

842   **Trinkaus E. 1997.** Appendicular robusticity and the paleobiology of modern human emergence.

843   *Proceedings of the National Academy of Sciences of the United States of America* **94**: 13367-

844   13373.

845   **Trinkaus E, Churchill SE, 1999.** Diaphyseal cross-sectional geometry of Near Eastern Middle

846   Palaeolithic humans: the humerus. *Journal of Archaeological Science* **26**: 173–184.

847   https://doi.org/10.1006/jasc.1998.0314

848   **Trinkaus E, Churchill SE, Ruff CB. 1994.** Postcranial robusticity in *Homo*. II: humeral bilateral

849   asymmetry and bone plasticity. *American Journal of Physical Anthropology* **93**: 1-34. DOI:

850   10.1002/ajpa.1330930102

851   **Trinkaus E, Stringer CB, Ruff CB, Hennessy RJ, Roberts MB, Parfitt SA.**

852   **1999.** Diaphyseal cross-sectional geometry of the Boxgrove 1 Middle Pleistocene human

853   tibia. *Journal of Human Evolution* **37**: 1-25. https://doi.org/10.1006/jhev.1999.0295

854   **Ungar PS, Grine FE, Teaford MF. 2006.** Diet in early *Homo*: a review of the evidence and a

855   new model of adaptive versatility. *Annual Review of Anthropology* **35**: 209-228.

856   **Von Koenigswald GHR. 1936.** Ein fossiler Hominide aus dem Altpleistocän Ostjavas. De

857   Ingenieur in Ned.-Indië, Mijnbouw & Geologie, De Mijningenieur **4**: 149-157.

858   **Von Koenigswald GHR. 1940.** Neue *Pithecanthropus* – Funde 1936-38, Eine Beitrag zur

859   Kenntnis der Praehominiden. Diens Mijnbow Ned. Indie, We. Meded. 28 Landsdrukkerij, pp.

860   1 – 205.

861 **Von Koenigswald GHR. 1951.** Introduction. In: Weidenreich, F., *Morphology of Solo Man*.

862 Anthropol. Pap. Am. Mus. Nat. Hist. 43, part 3, 211-221.

863 **Wallace IJ, Tommasini SM, Judex S, Garland Jr T, Demes B. 2012.** Genetic variations and

864 physical activity as determinants of limb bone morphology: An experimental approach using a

865 mouse model. *American Journal of Physical Anthropology* **148**:24-35.

866 **DOI:** 10.1002/ajpa.22028

867 **Walker A, Leakey RE. 1993.** The Nariokotome *Homo erectus* skeleton. Springer, Netherlands.

868 **Walker A, Zimmerman MR, Leakey REF. 1982.** A possible case of hypervitaminosis A in

869 *Homo erectus*. *Nature* **296**: 248-250.

870 **Warden SJ, Bogenschutz ED, Smith HD, Gutierrez AR. 2009.** Throwing induces substantial

871 torsional adaptation within the midshaft humerus of male baseball players. *Bone* **45**: 931-941.

872 https://doi.org/10.1016/j.bone.2009.07.075

873 **Weidenreich F. 1938.** Discovery of the femur and the humerus of *Sinanthropus pekinensis*.

874 *Nature* **141**: 614-617. DOI:10.1038/141614a0

875 **Weidenreich F. 1941.** *The extremity bones of* Sinanthropus pekinensis, Palaeontogia Sinica New

876 Series D 5.

877 **Weidenreich F. 1943.** *The skull of* Sinanthropus pekinenesis*: a comparative study on a primitive*

878 *hominid skull*. Palaeontogia Sinica New Series D **10**: 1-298.

879 **Weiner S, Xu Q, Goldberg P, Liu J, Bar-Yosef O. 1998.** Evidence for the use of fire at

880 Zhoukoudian, China. *Science* **281**: 251-253. DOI: 10.1126/science.281.5374.25

881 **Will M, Stock JT. 2015.** Spatial and temporal variation of body size among early *Homo*.

882   *Journal of Human Evolution* **82**: 15-33. https://doi.org/10.1016/j.jhevol.2015.02.009

883   **Williams EM, Gordon AD, Richmond BG. 2012.** Hand pressure distribution during Oldowan

884   stone tool production. *Journal of Human Evolution* **62**: 520-532.

885   https://doi.org/10.1016/j.jhevol.2012.02.005

886   **Woo J-K. 1964.** Mandible of *Sinanthropus lantianensis*. *Current Anthropology* 5, 98-101.

887   https://doi.org/10.1086/200457

888   **Woo J-K. 1966.** The skull of Lantian Man. Current Anthropology **7**: 83-86.

889   https://doi.org/10.1086/200664

890   **Woo J, Chia L. 1954.** New discoveries of *Sinanthropus pekinensis* in Choukoutien. *Acta*

891   *Palaeontologica Sinica* **2**: 267-288.

892   **Wood B. 1994.** Taxonomy and evolutionary relationships of *Homo erectus*. *Courier*

893   *Forschungsinstitut Senckenberg* **171**:159-165.

894   **Wu R, Dong X. 1982.** Preliminary study of *Homo erectus* from Hexian, Anhui. *Acta*

895   *Anthropologica Sinica* **1**: 2-13.

896   **Wu X. 1999.** Investigating the possible use of fire at Zhoukoudian, China. *Science* **283**: 299.

897   DOI: 10.1126/science.283.5400.299a

898   **Wu X, Poirier FE. 1995.** *Human evolution in China*. Oxford University Press, Oxford.

899   **Xie Y, Xing H, Xu J, Zhou B, Huang Y, Liu Y, Qu Z. 1985.** The sedimentary environment of

900   the Peking Man period. *Multidisciplinary study of the Peking Man site at Zhoukoudian*.

901   Science Press, Beijing, pp.185-215.

902   **Zaim Y, Ciochon RL, Polanski JM, Grine FE, Bettis EA III, Rizal Y, Franciscus RG, Larick**

903   **RR, Heizler M, Aswan Eaves KL, Marsh HE. 2011.** New 1.5 million-year-old *Homo*

904   *erectus* maxilla from Sangiran (Central Java, Indonesia). *Journal of Human Evolution* **61**: 363-

905   376. https://doi.org/10.1016/j.jhevol.2011.04.009

906   **Zhang SS. 2004.** *Beijing Annals: world Cultural Heritage Volume – the Peking Man Ruins*

907   *Annals*. Beijing Press, Beijing.

908   **Zhang Y, Tang ZW. 2007.** Discussion of the paleoenvironment of the Peking Man site. *Acta*

909   *Anthropologica Sinica* **26**: 34-44.

910   **Zhu RX, Potts R, Pan YX, Yao HT, Lü LQ, Zhao X, Gao X, Chen LW, Gao F, Deng CL.**

911   **2008.** Early evidence of the genus *Homo* in East Asia. *Journal of Human Evolution* **55**: 1075-

912   1085. https://doi.org/10.1016/j.jhevol.2008.08.005

913   **FIGURE CAPTIONS**

914   **Figure 1.** Zhoukoudian partial right humerus (PA64, Humerus III). A: anterior view of the

915   original fossils; B: posterior view of the original fossil; C: medial view of the original fossil; B:

916   lateral view of the original fossil; E:anterior view of the virtual reconstruction; F: posterior view

917   of the virtual reconstruction; G: medial view of the virtual reconstruction; H: lateral view of the

918   virtual reconstruction; I: a rendering (yellow) created from Humerus III is superimposed on a

919   mirrored rendering (light blue) created from the composite cast of Humerus II. Note general

920   correspondence in external shape and morphology between the midshaft regions of Humerus II

921   and Humerus III renderings. *Weidenreich (1941)* estimated maximum length of the Humerus II

922   rendering as 324.0 mm.

923   **Figure 2.** Humeral cross sections. A: Zhoukoudian Humerus III; B: Zhoukoudian Humerus II; C:

924   Tianyuan (right); D: Tianyuan (left); E: Datong-1; F: Datong-2; G: Datong-3; H: Datong-4; I:

925   Datong-5; J: Datong-6; K: Datong-7; L: Datong-8; M: Datong-9; N: Datong-10; O: Zhoukoudian

926   Humerus III; P: Zhoukoudian Humerus II. In the upper three rows, midshaft cross sections are

927   illustrated for Zhoukoudian Humerus II and Humerus III, Tianyuan 1 right and left humeri, and

928   Datong humeri (n = 10). The reconstructed cross section from the left humerus of Tianyuan 1 has

929   missing cortical bone estimated in green. In the bottom row, cross sections are illustrated for a

930   second, more distal location of Zhoukoudian Humerus II and Humerus III. Both estimated cross

931   sections from the Weidenreich composite cast of Humerus II have been mirrored for illustration

932   purposes. All midshaft cross sections from the Junziqing humeri (n = 23) are illustrated in Figure

933   S1.

934   **Figure 3.** Box plots of percent cortical area (%CA) in humeral midshaft cross sections reported

935   in Tables 1 and 2. Solid horizontal lines within boxes indicate median values, while height of

936   boxes indicates interquartile range (i.e., contains 50% of observations) and whiskers indicate the

937   observed highest and lowest values that do not exceed 1.5 times the interquartile range. Note that

938   the cross section for KNM-ER 1808 is an estimated 40% diaphyseal length rather than midshaft

939   *(Ruff, 2008)*. ZKD = Zhoukoudian; MPMH = Middle Paleolithic Modern Human; EUPMH =

940   Early Upper Paleolithic Modern Human; EELUPMH = East Eurasia Late Upper Paleolithic

941   Modern Human.

942   **Figure 4.** Box plots of standardized polar section modulus (Z_p) from the humeral midshaft (A)

943   and mid-distal (B) diaphysis reported in Tables 3-4 and Table S3, respectively. Standardization

944   procedures are reported in the methods section. The dotted lines illustrated for Zhoukoudian and

945   KNM-ER 1808 indicate the range of standardized properties using different combination of

946   humeral length and body mass. The solid horizontal line within the range indicates the value of

947   sZp standardized by average humeral length*average body mass. ZKD = Zhoukoudian.

Figure 1

Zhoukoudian partial right humerus (PA64, Humerus III)

Figure 1. Zhoukoudian partial right humerus (PA64, Humerus III). A: anterior view of the original fossils; B: posterior view of the original fossil; C: medial view of the original fossil; B: lateral view of the original fossil; E: anterior view of the virtual reconstruction; F: posterior view of the virtual reconstruction; G: medial view of the virtual reconstruction; H: lateral view of the virtual reconstruction; I: a rendering (yellow) created from Humerus III is superimposed on a mirrored rendering (light blue) created from the composite cast of Humerus II. Note general correspondence in external shape and morphology between the midshaft regions of Humerus II and Humerus III renderings. *Weidenreich (1941)* estimated maximum length of the Humerus II rendering as 324.0 mm.

Note: Auto Gamma Correction was used for the image. This only affects the reviewing manuscript. See original source image if needed for review.

Figure 2

Humeral cross sections

Figure 2. Humeral cross sections. A: Zhoukoudian Humerus III; B: Zhoukoudian Humerus II; C: Tianyuan (right); D: Tianyuan (left); E: Datong-1; F: Datong-2; G: Datong-3; H: Datong-4; I: Datong-5; J: Datong-6; K: Datong-7; L: Datong-8; M: Datong-9; N: Datong-10; O: Zhoukoudian Humerus III; P: Zhoukoudian Humerus II. In the upper three rows, midshaft cross sections are illustrated for Zhoukoudian Humerus II and Humerus III, Tianyuan 1 right and left humeri, and Datong humeri (n = 10). The reconstructed cross section from the left humerus of Tianyuan 1 has missing cortical bone estimated in green. In the bottom row, cross sections are illustrated for a second, more distal location of Zhoukoudian Humerus II and Humerus III. Both estimated cross sections from the Weidenreich composite cast of Humerus II have been mirrored for illustration purposes. All midshaft cross sections from the Junziqing humeri (n = 23) are illustrated in Figure S1.

Note: Auto Gamma Correction was used for the image. This only affects the reviewing manuscript. See original source image if needed for review.
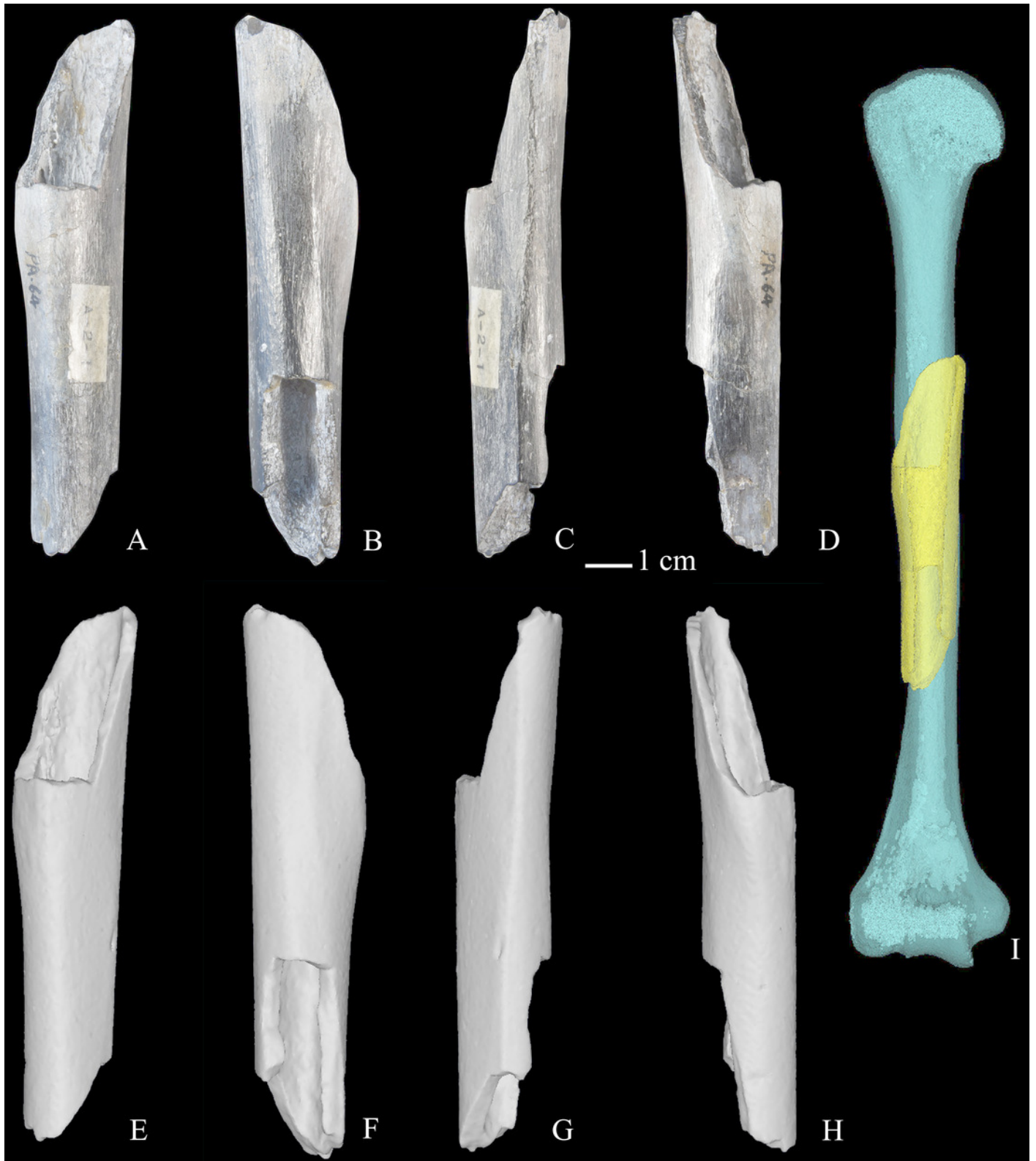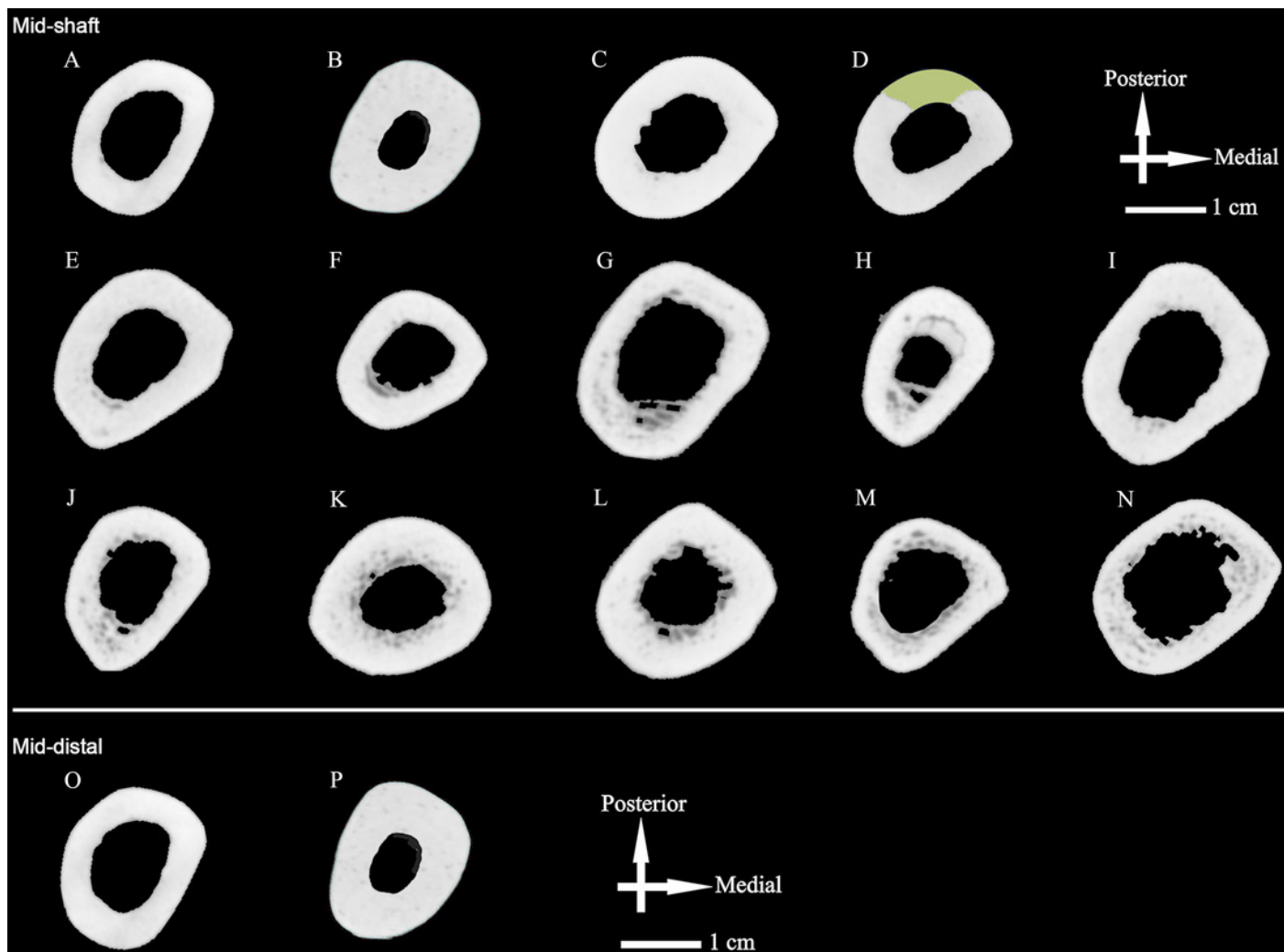
Figure 3

Box plots of percent cortical area (%CA) in humeral midshaft cross sections

Figure 3. Box plots of percent cortical area (%CA) in humeral midshaft cross sections reported in Tables 1 and 2. Solid horizontal lines within boxes indicate median values, while height of boxes indicates interquartile range (i.e., contains 50% of observations) and whiskers indicate the observed highest and lowest values that do not exceed 1.5 times the interquartile range. Note that the cross section for KNM-ER 1808 is an estimated 40% diaphyseal length rather than midshaft *(Ruff, 2008)*. ZKD = Zhoukoudian; MPMH = Middle Paleolithic Modern Human; EUPMH = Early Upper Paleolithic Modern Human; EELUPMH = East Eurasia Late Upper Paleolithic Modern Human.
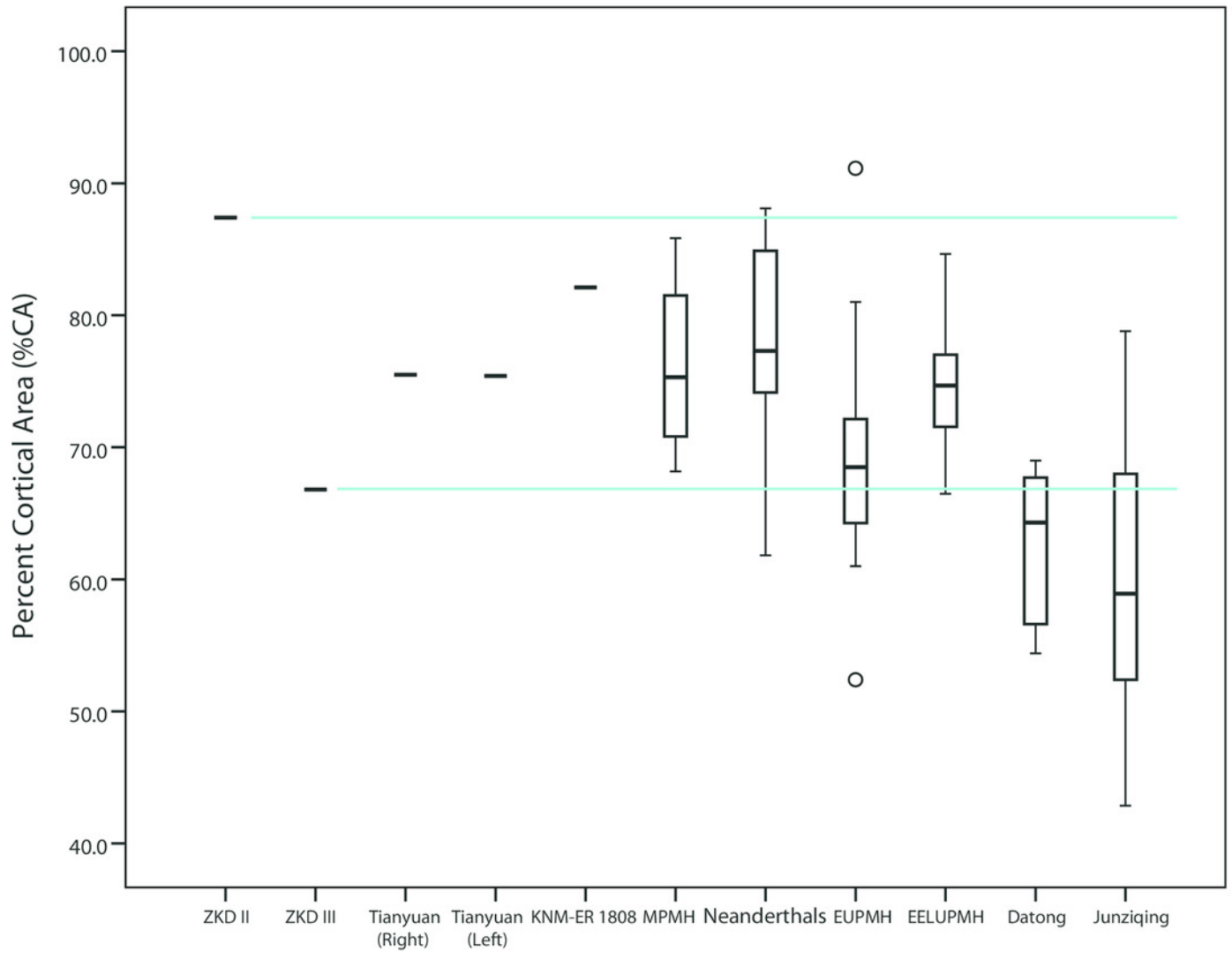
Figure 4

Box plots of standardized polar section modulus (Z_p) from the humeral midshaft (A) and mid-distal (B) diaphysis

Figure 4. Box plots of standardized polar section modulus (Z_p) from the humeral midshaft (A) and mid-distal (B) diaphysis reported in Tables 3-4 and Table S3, respectively. Standardization procedures are reported in the methods section. The dotted lines illustrated for Zhoukoudian and KNM-ER 1808 indicate the range of standardized properties using different combination of humeral length and body mass. The solid horizontal line within the range indicates the value of sZp standardized by average humeral length*average body mass. ZKD = Zhoukoudian.

Table 1(on next page)

Midshaft humeral unstandardized properties of Zhoukoudian right humerus (III) and comparative samples

Table 1. Midshaft humeral unstandardized properties of Zhoukoudian right humerus (III) and comparative samples.

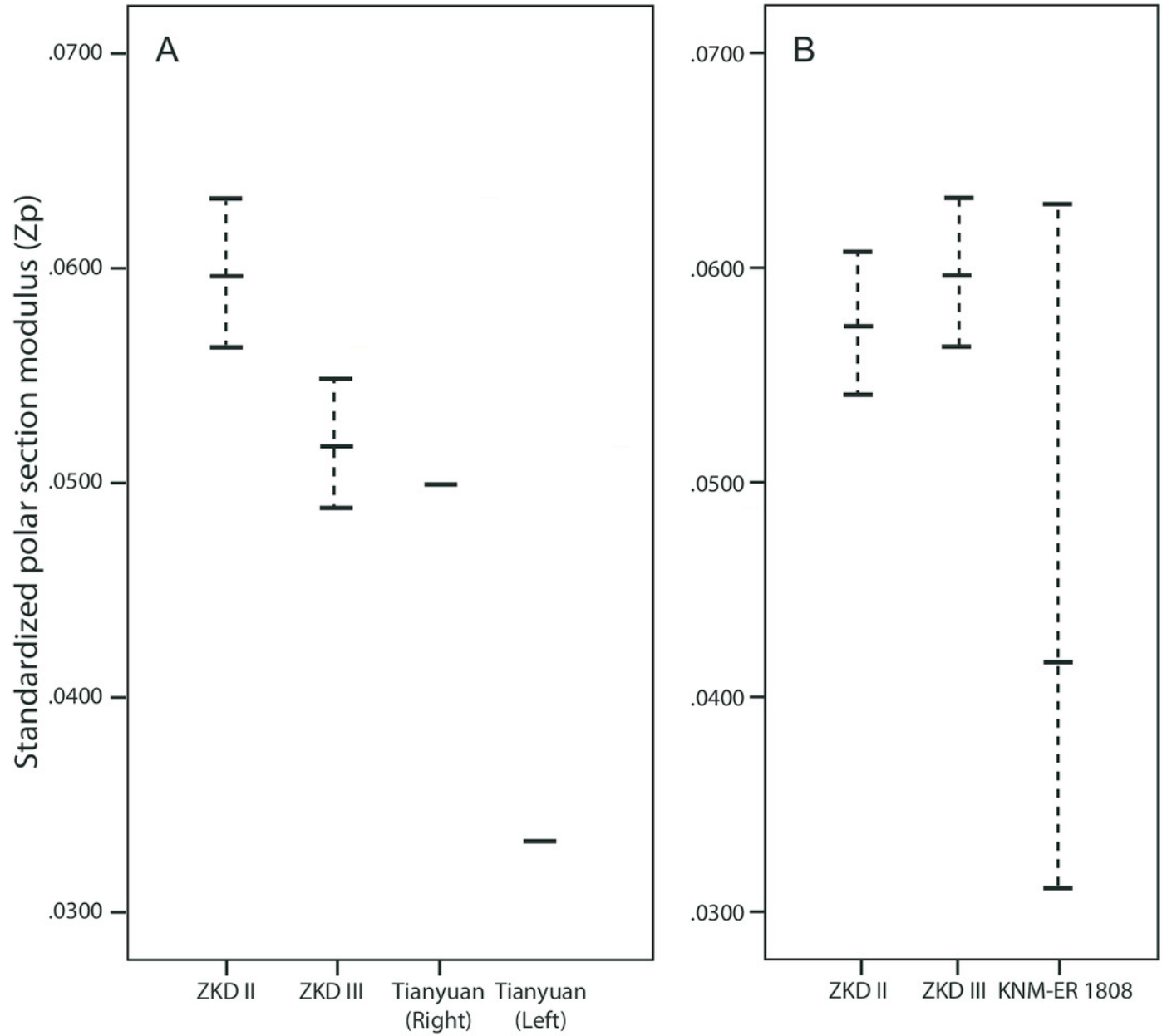|		Length (mm)	Body Mass (kg)	TA (mm²)	CA (mm²)	%CA	I_{max} (mm⁴)	I_{min} (mm⁴)	Z_{max} (mm³)	Z_{min} (mm³)	J (mm⁴)	Z_p (mm³)
Zhoukoudian III*[1]		307.4- 324.0	53.6 ± 1.7	250	167	66.8	5959	3307	579	415	9266	875
KNM-ER 1808[2]		350.0	60.2 ± 20.4	240	197	82.1	5212	3891	503	457	9103	877
Tianyuan 1*[3]		327.4	85.1	330	249	75.5	10561	6345	912	684	16906	1391
Middle Paleolithic Modern Human[4] (n=4 for length, TA, CA, I_x, and I_y, n=2 for body mass, n=5 for I_{max}, I_{min}, and J)	Mean	358.3	66.1	303.5	235.3	76.2	8152	5216	-	-	13368	-
	S.D.	20.5	3.9	80.5	81.3	7.4	4452	2985	-	-	7395	-
	Min	329.0	63.3	190.7	130.0	68.2	3591	1946	-	-	5537	-
	Max	375.0	68.8	381.4	327.4	85.8	14567	8834	-	-	23401	-
Neanderthals[4] (n=12 for length, n=9 for body mass, n=12 for TA, CA, I_x, and I_y, n=14 for I_{max} and I_{min}, n=15 for J)	Mean	301.6	71.5	314.8	244.5	77.8	9373	5444	-	-	14945	-
	S.D.	20.6	10.1	79.3	65.6	7.7	4062	2479	-	-	6246	-
	Min	262.0	59.9	183.3	125.3	61.8	3705	1887	-	-	5592	-
	Max	335.5	85.5	426.0	365.9	88.1	14787	9757	-	-	24544	-
Early Upper Paleolithic Modern Human[4] (n=17 for length, n=13 for body mass, n=14 for TA, CA, I_x, and I_y, n=22 for I_{max}, I_{min}, and J)	Mean	332.6	69.0	330.7	227.4	69.6	9317	6094	-	-	15411	-
	S.D.	25.9	7.8	73.4	48.6	9.2	3558	2253	-	-	5716	-
	Min	284.0	55.7	181.5	143.0	52.4	3210	2207	-	-	5417	-
	Max	371.0	82.5	444.2	316.8	91.1	17592	10579	-	-	27736	-
East Eurasia Late Upper Paleolithic Modern Human[4] (n=9 for length, n=8 for body mass, n=10 for TA, CA, I_x, I_y, I_{max}, I_{min}, and J)	Mean	274.3	51.4	232.1	172.5	74.7	5612	2937	-	-	8549	
	S.D.	18.1	9.9	30.5	18.7	5.1	1570	774	-	-	2251	
	Min	252.0	42.3	189.5	153.6	66.5	3671	2132	-	-	5803	
	Max	311.0	70.5	283.1	218.0	84.6	8331	4486	-	-	12817	
Datong (n=10)[5]	Mean	305.8	-	308	193	62.8	8660	5360	742	548	14020	1143
	S.D.	18.2	-	69	46	5.7	3743	2254	251	196	5951	395
	Min	272.4	-	210	131	54.4	4134	2166	401	307	6336	601
	Max	328.0	-	397	258	69.0	14107	8751	1072	831	22858	1715
Junziqing (n=23)[5]	Mean	286.2	-	268	161	59.7	6199	3958	565	451	10157	915
	S.D.	17.5	-	50	44	10.8	2514	1663	190	143	4132	308
	Min	262.9	-	193	90	42.9	2678	1722	288	255	4632	497
	Max	327.7	-	384	243	78.8	11814	7540	988	738	18877	1571

2   *Estimated cross section location due to incomplete length. [1]Maximum length of the left Zhoukoudian Humerus II was reported by *Weidenreich*

3   *(1941)* to be 324.0 mm. We estimated maximum length as 307.4 mm using a regression analysis of the distance between the deltoid tuberosity and

4   the proximal margin of the olecranon fossa against maximum length on our comparative sample of Datong and Junziqing modern *Homo sapiens* (n

5   = 33; see Text S1 in the Supporting Information). In order to be conservative, we use both estimates to provide a range of standardized values for

6   Zhoukoudian humeri about a mean value (315.7 mm). In order to standardize cross-sectional properties, we used maximum length estimates of the

7   reconstructed left Zhoukoudian Humerus II as proxies for maximum length estimates of the partial right Zhoukoudian Humerus III. [2]Cross-

8   sectional data for a 40% length section published by *Ruff (2008: Fig. 1)*. We used a rough approximation of 350.0 mm for humeral

9   length (*Ruff, 2008; pers. comm*). [3]In order to standardize cross-sectional properties, but acknowledging substantial bilateral asymmetry in their

10   cross-sectional properties, we chose to use biomechanical length of the left Tianyuan 1 humerus (327.4 mm: *Shang & Trinkaus, 2010*) as a proxy

11   for length of the right Tianyuan 1 humerus. [4]Data from *Churchill (1994)*, *Trinkaus et al. (1994)*, *Trinkaus & Churchill (1999)*, *Crevecoeur (2008)*,

12   and *Sparacello et al. (2016)*. [5]Amongst the recent modern human comparative sample, the distal-most point of the deltoid tuberosity was between

13   43 and 53% shaft length, with the majority of specimens falling between 46 and 51%.

Table 2(on next page)

Midshaft humeral unstandardized properties of Zhoukoudian left humerus (II) and comparative samples

1 **Table 2. Midshaft humeral unstandardized properties of Zhoukoudian left humerus (II) and comparative samples.**

		Length	Body mass	TA	CA	%CA	I_{max}	I_{min}	Z_{max}	Z_{min}	J	Z_p
		(mm)	(kg)	(mm²)	(mm²)		(mm⁴)	(mm⁴)	(mm³)	(mm³)	(mm⁴)	(mm³)
Zhoukoudian II*[1]		307.4-324.0	53.6 ± 1.7	261	228	87.4	6985	4143	640	518	11128	1009
Tianyuan 1*[2]		327.4	85.1	252	190	75.4	5931	3868	603	463	9799	928
Middle Paleolithic Modern Human[3] (n=2 for length, body mass, TA, CA, I_x, and I_y, n=3 for I_{max}, I_{min}, and J)	Mean	353.3	68.9	283.1	217.0	76.8	5894	4088	-	-	9981	-
	S.D.	30.8	0.1	5.2	56.9	21.5	2021	1619	-	-	3618	-
	Min	331.5	68.8	279.4	176.7	61.6	3564	2287	-	-	5851	-
	Max	375.0	69.0	286.7	257.2	92.1	7170	5421	-	-	12591	-
Neanderthals[3] (n=5 for length, n=4 for body mass, n=7 for TA and CA, n=6 for I_x and I_y, n=8 for I_{max} and I_{min}, n=9 for J)	Mean	314.4	79.1	256.0	197.8	77.6	7879	4173	-	-	12112	-
	S.D.	13.4	9.7	44.0	29.3	3.6	2863	1658	-	-	4199	-
	Min	299	64.8	203.5	170.7	73.9	4629	2250	-	-	6879	-
	Max	334	85.5	341.1	251.9	84.2	12020	6411	-	-	18250	-
Early Upper Paleolithic Modern Human[3] (n=20 for length, n=15 for body mass, n=17 for TA, CA, I_x, and I_y, n=22 for I_{max} and I_{min}, n=23 for J)	Mean	326.5	68.4	298.6	198.6	67.1	7119	4799	-	-	12138	-
	S.D.	21.0	7.7	46.1	29.5	8.9	1965	1315	-	-	2978	-
	Min	288.0	54.3	199.8	133.0	47.9	3670	2148	-	-	5895	-
	Max	370.0	82.5	394.1	246.7	83.0	10701	7316	-	-	17605	-
East Eurasia Late Upper Paleolithic Modern Human[3] (n=7 for length, n=5 for body mass, n=10 for TA, CA, I_x, I_y, I_{max}, I_{min}, and J)	Mean	273.1	53.2	227.6	168.4	74.2	5106	2972	-	-	8078	-
	S.D.	20.3	10.5	33.8	27.9	7.6	1463	955	-	-	2395	-
	Min	250.0	42.3	186.7	138.8	65.7	3437	1900	-	-	5587	-
	Max	311.0	70.5	281.8	225.1	86.5	7432	4724	-	-	11968	-

2

3 *Estimated cross section location due to incomplete length. [1]Maximum length of the left Zhoukoudian Humerus II was reported by *Weidenreich*

4 *(1941)* to be 324.0 mm. We estimated maximum length as 307.4 mm using a regression analysis of the distance between the deltoid tuberosity and

5   the proximal margin of the olecranon fossa against maximum length on our comparative sample of Datong and Junziqing modern *Homo sapiens* (n

6   = 33; see Text S1 in the Supporting Information). In order to be conservative, we use both estimates to provide a range of standardized values for

7   Zhoukoudian humeri about a mean value (315.7 mm). We estimated cross-sectional properties of Humerus II from its periosteal contour, and a

8   radiograph published by *Weidenreich* (*1941: Fig. 58 D*; see Text S3 in the Supporting Information. [2]Data from *Shang &Trinkaus (2010)*. [3]Data

9   from *Churchill (1994)*, *Trinkaus et al. (1994)*, *Trinkaus & Churchill (1999)*, *Crevecoeur (2008)*, and *Sparacello et al. (2016)*.

Table 3(on next page)

Midshaft humeral standardized properties (by estimated body mass x maximum length) of Zhoukoudian right humerus (III) and comparative samples

Table 3. Midshaft humeral standardized properties (by estimated body mass x maximum length) of Zhoukoudian right humerus (III) and comparative samples*.

	BM	HL	sI_{max}	sI_{min}	sZ_{max}	sZ_{min}	sJ	sZ_p
ZKD Humerus III	53.6	307.4	0.362	0.201	0.035	0.025	0.562	0.053
	53.6	**315.7**	**0.352**	**0.195**	**0.034**	**0.024**	**0.548**	**0.052**
	53.6	324.0	0.343	0.190	0.033	0.024	0.534	0.050
	55.3	307.4	0.351	0.195	0.035	0.025	0.545	0.051
	55.3	315.7	0.341	0.189	0.034	0.025	0.531	0.050
	55.3	324.0	0.333	0.185	0.033	0.024	0.517	0.049
	51.9	307.4	0.374	0.207	0.034	0.024	0.581	0.055
	51.9	315.7	0.364	0.202	0.033	0.024	0.567	0.053
	51.9	324.0	0.354	0.197	0.032	0.023	0.551	0.052
KNM-ER 1808	**60.2**	**350**	**0.247**	**0.185**	**0.024**	**0.022**	**0.432**	**0.042**
	80.6	350	0.185	0.138	0.018	0.016	0.323	0.031
	39.8	350	0.374	0.279	0.036	0.033	0.653	0.063
Tianyuan 1	85.1	327.4	0.379	0.228	0.033	0.025	0.607	0.050
Middle Paleolithic Modern Human (n=2)		Mean	0.339	0.282	-	-	0.682	-
		S.D.	0.099	0.047	-	-	0.146	-
		Min	0.329	0.249	-	-	0.579	-
		Max	0.469	0.315	-	-	0.785	-
Neanderthals (n=8 for sTA, sCA, sImax, and sImin, n=9 for sJ)		Mean	0.420	0.244	-	-	0.682	-
		S.D.	0.165	0.117	-	-	0.265	-

	Min	0.222	0.100	-	-	0.322	-
	Max	0.668	0.441	-	-	1.109	-
Early Upper Paleolithic Modern Human (n=7 for sTA and sCA, n=13 for sImax, sImin, and sJ)	Mean	0.402	0.266			0.668	-
	S.D.	0.094	0.062			0.152	-
	Min	0.283	0.195			0.478	-
	Max	0.587	0.400			0.926	-
East Eurasian Late Upper Paleolithic Modern Human (n=7)	Mean	0.414	0.217			0.631	-
	S.D.	0.109	0.030			0.132	-
	Min	0.321	0.175			0.509	-
	Max	0.636	0.259			0.875	-

*Humeral lengths (HL), body mass (BM), and original properties used in calculating the standardized properties are reported in Table 1, except for ZKD humeri, where three length estimates (307.4, 315.7, and 324.0 mm) and three body mass estimates (Average + 1SD = 55.3 kg, Average = 53.6 kg, Average – 1SD = 51.9 kg) were used. Three body mass estimates of KNM-ER 1808 (Average + 1SD = 80.6 kg, Average = 60.2 kg, Average – 1SD = 39.8 kg) were also used. Bold font indicates values standardized by average length and body mass estimates.

Table 4(on next page)

Midshaft humeral standardized properties (by body mass x maximum length) of Zhoukoudian left humerus (II) and comparative samples

Table 4. Midshaft humeral standardized properties (by body mass x maximum length) of Zhoukoudian left humerus (II) and comparative samples*.

	BM	HL	sI_{max}	sI_{min}	sZ_{max}	sZ_{min}	sJ	sZ_p
ZKD Humerus II	53.6	307.4	0.424	0.251	0.039	0.031	0.675	0.061
	53.6	**315.7**	**0.413**	**0.245**	**0.038**	**0.030 6**	**0.658**	**0.060**
	53.6	324.0	0.402	0.239	0.037	0.030	0.641	0.058
	55.3	307.4	0.411	0.244	0.038	0.030	0.655	0.059
	55.3	315.7	0.400	0.237	0.037	0.030	0.637	0.058
	55.3	324.0	0.390	0.231	0.036	0.029	0.621	0.056
	51.9	307.4	0.438	0.260	0.040	0.032	0.698	0.063
	51.9	315.7	0.426	0.253	0.039	0.032	0.679	0.062
	51.9	324.0	0.415	0.246	0.038	0.031	0.662	0.060
Tianyuan 1	85.1	327.4	0.213	0.139	0.022	0.017	0.352	0.033
Middle Paleolithic Modern Human (n=2)		Mean	0.291	0.207			0.498	
		S.D.	0.031	0.043			0.074	
		Min	0.269	0.177			0.446	
		Max	0.313	0.237			0.550	
Neanderthals (n=4 for sTA, sCA, and sJ, n=3 for sI_{max} and sI_{min},)		Mean	0.363	0.182			0.534	
		S.D.	0.186	0.102			0.237	
		Min	0.253	0.118			0.375	
		Max	0.578	0.300			0.877	
Early Upper Paleolithic Modern Human (n=9 for sTA and sCA,		Mean	0.300	0.201			0.506	
		S.D.	0.05	0.04			0.09	

n=14 for sI_{max} and sI_{min}, n=15 for sJ)		9	0	2
	Min	0.202	0.129	0.355
	Max	0.405	0.272	0.674
East Eurasian Late Upper Paleolithic Modern Human (n=5)	Mean	0.313	0.186	0.500
	S.D.	0.044	0.035	0.077
	Min	0.256	0.139	0.416
	Max	0.353	0.215	0.566

*Humeral lengths (HL), body mass (BM), and original properties used in calculating the standardized properties are reported in Table 2, except for ZKD humeri, where three length estimates (307.4, 315.7, and 324.0 mm) and three body mass estimates (Average + 1SD = 55.3 kg, Average = 53.6 kg, Average – 1SD = 51.9 kg) were used. Bold font indicates values standardized by average length and body mass estimates.